Acta Zoologica

Published for The Royal Swedish Academy of Sciences and The Royal Danish Academy of Sciences and Letters

Acta Zoologica (Stockholm) **90**: 301–325 (October 2009) doi: 10.1111/j.1463-6395.2008.00356.x

Chondrocranium and skeletal development of *Phrynops hilarii* (Pleurodira: Chelidae)

Paula Bona[1] and Leandro Alcalde[2]

[1]Museo de La Plata, Paseo del Bosque s/n. CP1900, La Plata, Buenos Aires, Argentina; [2]Instituto de Limnología Dr R. A. Rínguelet Avda, Calchaquí Km 23.5, CP1888, Florencio Varela, Buenos Aires, Argentina

Keywords:
Phrynops, Testudines, Chelidae, skeletal development, chondrocranium

Accepted for publication:
22 June 2008

Abstract

Bona, P. and Alcalde, L. 2009. Chondrocranium and skeletal development of *Phrynops hilarii* (Pleurodira: Chelidae). — *Acta Zoologica* (Stockholm) **90**: 301–325

The present study represents the first comprehensive contribution to the knowledge of the skeletal development of a pleurodiran turtle, *Phrynops hilarii* (Pleurodira, Chelidae). The most remarkable features found are: (1) absence of ascending process on pterygoquadrate cartilage; (2) presence of ossification centres for the epiotics; (3) as in other pleurodirans, dorsal ribs IX and X are 'sacralized'; (4) contact between ilium and carapace occurs later in ontogenetic development; (5) suture between ischia, pubes and plastron occurs in posthatching specimens; (6) contrary to previous interpretations, the phalangeal formula of the pes of *P. hilarii* is 2 : 3 : 3 : 3 : 5; (7) the hooked bone represents the fifth metatarsal.

Paula Bona, Departamento de Paleontología Vertebrados, Museo de La Plata, Paseo del Bosque s/n, 1900, Argentina. E-mail: pbona@fcnym.unlp.edu.ar

Introduction

The Pleurodira, commonly known as 'side-necked turtles', are one of the major monophyletic assemblages of extant turtles. This group comprises two major clades (Joyce 2007), both distributed in the southern hemisphere: the pelomedusoids, restricted to Africa, Madagascar and South America (de Broin 1988), and the Chelidae, distributed in Australasia and South America. Although the monophyly of both Pleurodira and Chelidae is widely accepted, the phylogenetic relationships within each clade remain controversial (Boulenger 1889; Burbidge *et al.* 1974; Gaffney 1977; Gaffney and Meylan 1988; Seddon *et al.* 1997; Shaffer *et al.* 1997; Georges *et al.* 1998; Noonan 2000; Fujita *et al.* 2003; Bona and de la Fuente 2005; Joyce 2007).

Furthermore, the species studied here, *Phrynops hilarii*, belongs to *Phrynops* (*sensu lato*), a group of chelids endemic to South America that includes taxa (e.g. *Phrynops*, *Mesoclemmys*, and *Batrachemys*) with unsettled interrelationships (Shaffer *et al.* 1997; Seddon *et al.* 1997; Georges *et al.* 1998; McCord *et al.* 2001).

Morphology is a central topic in practically all aspects of evolutionary biology. Morphological description and comparisons across taxa allow character delimitation for use in phylogenetic reconstruction, provide morphological support of molecularly based clades, and the morphological patterns are central to understanding the expression of regulatory genes at different structural levels (Holmgren 1933; Shubin and Alberch 1986; Fabrezi and Alberch 1996; Mabee 2000; Gilbert *et al.* 2001). Although the anatomical and morphological variability of turtles was studied by several authors (e.g. Boulenger 1889; Rabl 1910; Holmgren 1933; Zug 1971; Walker 1973; Gaffney 1990; Rieppel 1993a; Gilbert *et al.* 2001; Crumly and Sánchez-Villagra 2004; Sheil 2005; Bever 2008 among others), only a few works contain comprehensive descriptions of the development of the entire skeletal system (Rieppel 1993a; Sheil 2003, 2005); this paucity of information is particularly evident for the cranial and postcranial ontogeny of pleurodiran turtles. This lack of data on pleurodiran skeletal development is relevant because most interpretations of homology, skeletal patterns and other cranial and postcranial features suggested for 'Testudines', are based largely on cryptodiran anatomy (Gaffney 1979; Rieppel 1994; works cited therein). Additionally, the study of skeletal morphogenesis in pleurodirans contributes to establishing the patterns of chondrification and ossification and their variability among turtles, the structural patterns of different skeletal elements, and even to understanding the morphological changes that have occurred during the evolution of turtles. For example,

Sánchez-Villagra *et al.* (2007) pointed out the need for studies concerning autopodial morphology and its development in Pleurodira. These authors highlighted the importance of this type of character for cladistic-systematic treatments of this group, because several autopodial synapomorphies were identified at different taxonomic levels (family, genus and species).

The present work is the first comprehensive description of the osteological development for a pleurodiran turtle (*P. hilarii*), and has the following goals: (1) to increase our understanding of morphological variation in turtles; (2) to discuss primary homologies of several cranial and postcranial elements; and (3) to propose structural and developmental patterns for different elements of the axial and appendicular skeleton of this species.

Materials and Methods

Nineteen *P. hilarii* embryos (stages 19, 21, 22, 23, 25 and 26) and one subadult (juvenile, lacking external sexual dimorphism) were double-stained and cleared according to the technique of Taylor and Van Dyke (1985). Additionally, the dry skeletons of two adults were also studied. All specimens are housed at the herpetological collections of the Museo de La Plata (La Plata, Buenos Aires, Argentina – MLP R) and Fundación Miguel Lillo (Tucumán, Argentina – FML) (see Appendix I). Embryos were staged according to the table of Greenbaum and Carr (2002). This was chosen for two reasons: first, the Greenbaum and Carr (2002) staging criteria allow comparisons among distant taxa of turtles; and second, although novel, these criteria are described in the context of the widely used sequence of Yntema (1968).

Observations, drawings and measurements were made under a stereoscopic microscope (Carl Zeiss Jena) equipped with camera lucida and micrometric ocular (± 0.1 mm). Subadults and adults were measured using digital calipers (± 0.1 mm). Reconstruction of relative ossification sequences was based on the first stage at which each element retained Alizarine.

Intrastage variation, when present, was taken into account to describe the patterns for skeletal units. Nomenclature is used according to the following sources: ossification mechanism (Hall 2005), cartilaginous neurocranium and mandibular arch (Kunkel 1912), hyoid arch (Schumacher 1973), osteocranium and its foramina (Gaffney 1979), vertebrae (Hoffsteter and Gasc 1969), carapace and plastron (Burke 1989), pectoral girdle (Vickaryous and Hall 2006), pelvic girdle (Romer 1956) and fore- and hindlimb (Burke and Alberch 1985).

With respect to axial development, carapace neural plates were numerated according to the dorsal vertebra in contact with each one (e.g. first neural plate is the one that contacts the first dorsal vertebra), and the term 'transverse processes' was used for the lateral projections of the vertebral body, not considering the inclusion of a rib.

To describe possible types of relationships between bones (in particular between skull bones) during their development, we use three terms: contact, overlap and suture. The first designates two adjacent bones that contact each other along their margins. The second describes a condition in which the margin of one bone grows over that of an adjacent element. Finally, 'suture' designates cases in which formerly overlapping bones become firmly attached to each other through common osseous development.

Nineteen eggs were obtained from different people that possess captive breeding populations of adult *P. hilarii* from unknown localities. All eggs were carried to the laboratory and placed in open plastic boxes (10 × 10 × 20 cm, five eggs each), using a substrate 1 : 1 of vermiculite and water. The temperature ranged from 25 to 28 °C, with 12 h of light per day. Embryos were 'anaesthetized' using a solution of ethanol 70% and benzocaine, and then fixed in 5% buffered formalin.

Results

Chondrocranium

The chondrocranium was described using a stage 19 embryo (MLP R. 5321). This was the earliest stage available in the developmental series of *P. hilarii* studied herein. The few bones present at this stage are small, whereas the chondrocranium is fully formed (see Fig. 1).

Nasal capsule. The nasal capsules are rounded with a small anterior process placed ventral to the fenestra narina (Fig. 1C). The fenestra narina is visible only in a frontal view. The nasal capsules represent approximately one-quarter of the total neurocranium length. The lateral wall of each capsule is formed by the antorbital plane. The epiphanial foramen opens dorsolaterally in the antorbital plane and transmits the ramus lateralis of the profundus nerve (Fig. 1A,C). The antorbital plane lacks the ectochoanal and rostral processes. Each capsule is open to the orbital region by means of an ample orbitonasal fenestra. This fenestra is limited laterally by the free posterior margin of the antorbital plane and medially by the sphenoethmoidal commissure. The orbitonasal fenestra transmits the posterior nasal artery and is tapered by the nasal capsule in a lateral view. Also in a lateral view, the sphenoethmoidal commissure is obscured by the great development of the nasal capsule. The sphenoethmoidal commissure is evident in a dorsal view at each side of the anterior end of the supraseptal plane. This commissure along with the nasal septum delimits an ample olfactory foramen for the olfactory nerve at each side (Fig. 1A). The floor of each capsule is extensively perforated by the choana (Fig. 1B). Each kidney-shaped choana is limited by the ventral margin of the antorbital plane, the paraseptal plane and the lamina transversalis. The prepalatine foramina open at both sides of the nasal septum and transmit the anterior

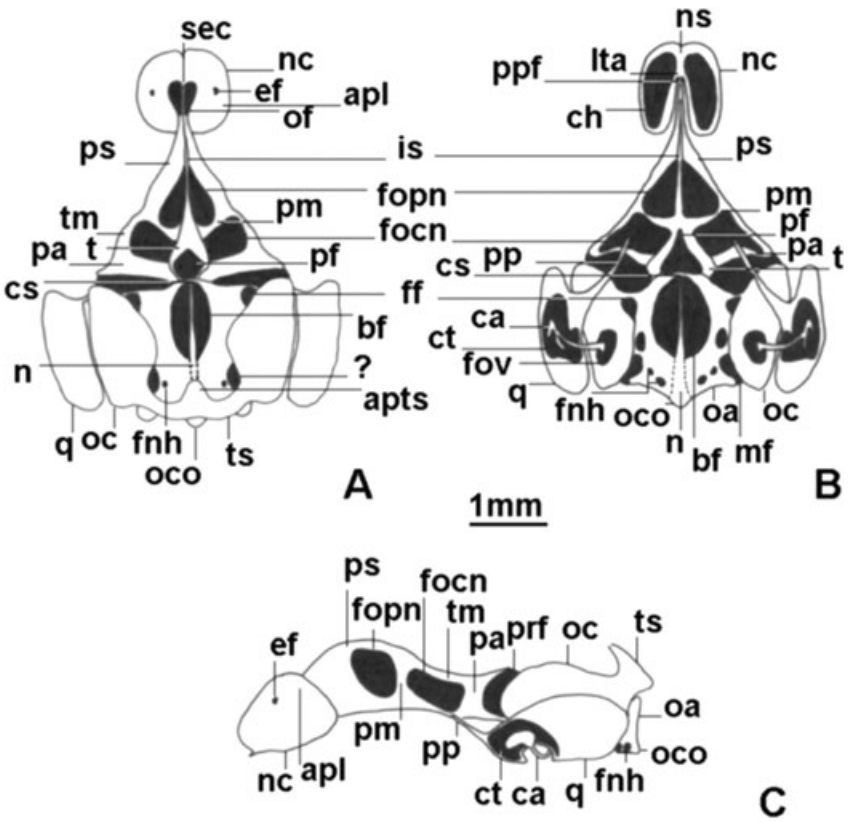

Fig. 1—Chondrocranium of *Phrynops hilarii* at stage 19 (MLP R. 5321). —**A**. Dorsal, —**B**. ventral, and —**C**. lateral views. Black areas represent cranial foramina and openings. Abbreviations: apl, antorbital plane; apts, anterior process of tectum synoticum; bf, basicranial fenestra; ca, columella auris; ch, choana; cs, crista sellaris; ct, cavum tympani; ef, epiphanial foramen; ff, foramen nervi facialis; fnh, foramen nervi hypoglossi; focn, foramen for oculomotor nerve; fopn, foramen for optic nerve; fov, fenestra ovalis; is, interorbital septum; lta, lamina transversalis; mf, metotic fissure; n, notochord swelling; nc, nasal capsule; ns, nasal septum; oa, occipital arch; oc, otic capsule; oco, occipital condyle; of, olfactory foramen; pa, pila antotica; pf, pituitary fenestra; pm, pila metoptica; ppf, prepalatine foramen; pp, pterygoid process of pterygoquadrate cartilage; prf, prootic fenestra; ps, planum supraseptale; q, quadrate cartilage; sec, sphenoethmoidal commissure; t, trabecula; tm, taenia marginalis; ts, tectum synoticum.

nasal artery. These foramina are delimited laterally by the paraseptal plane (Fig. 1B).

Orbitotemporal region. The well-chondrified trabeculae form the lateral margins of a pentagonal pituitary fenestra (Fig. 1A). The latter is separated from the basicranial fenestra by the crista sellaris. The trabeculae are joined anteriorly to the pituitary fenestra forming the intertrabecular plane. The metoptic pillars and the interorbital septum arise upon the intertrabecular plane (Fig. 1A,B). The interorbital septum represents a poorly chondrified area anterior to the optic foramen for the optic nerve. The interorbital septum is dorsally curved forming a convex supraseptal plane, which meets the sphenoethmoidal commissure anteriorly and projects posterodorsally forming the taenia tecti marginalis until contacting the antotic pillar. The taenia tecti marginalis closes the oculomotor foramen for the oculomotor nerve (Fig. 1A,C). The metoptic pillar separates the oculomotor foramen from the optic foramen. The ophthalmic artery foramen is represented by an ingression of the oculomotor foramen between the floor of the optic foramen and the intertrabecular plane. The antotic pillar is the most posterior of the cartilages in the orbital region and delimits the anterior margin of the prootic fenestra for the trigeminus nerve (Fig. 1C). This pillar is approximately shorter than the metoptic pillar, and it is more expanded dorsally than at its base.

Otic capsule. The kidney-shaped otic capsules occupy approximately one-third of the total neurocranium length and are firmly attached to the parachordal cartilages. The capsules are lateroventrally pierced by the fenestra ovalis for the stapedial footplate (Fig. 1B). Near to the anterior margin of the fenestra ovalis opens the foramen for the facial nerve. This opening is closed dorsally by a cartilaginous commissure that separates the foramen from the prootic fenestra (Fig. 1B). The skull roof is formed by the tectum synoticum that joins the posterior halves of the otic capsules to each other (Fig. 1A). The middle portion of the tectum synoticum projects anteriorly.

Basal plate and occipital region. The occipital arches rise posterior to the otic capsules from the caudal end of the parachordal cartilages (Fig. 1B,C). The dorsally open metotic fissure lies between the otic capsule and the occipital arch (Fig. 1B). This fissure is the common opening for the glossopharyngeal and vagus nerves. The hypoglossal nerve passes through two foramina at the base of each occipital arch (Fig. 1B). The right and left occipital arches form the condyle when they meet ventrally. The anterior region of the basicranial fenestra presents an oval perforation of unknown function. This perforation is twice the size of the pituitary fenestra (Fig. 1B).

Palatoquadrate and columella. The palatoquadrate is formed posteriorly by a massive cartilaginous quadrate placed lateral

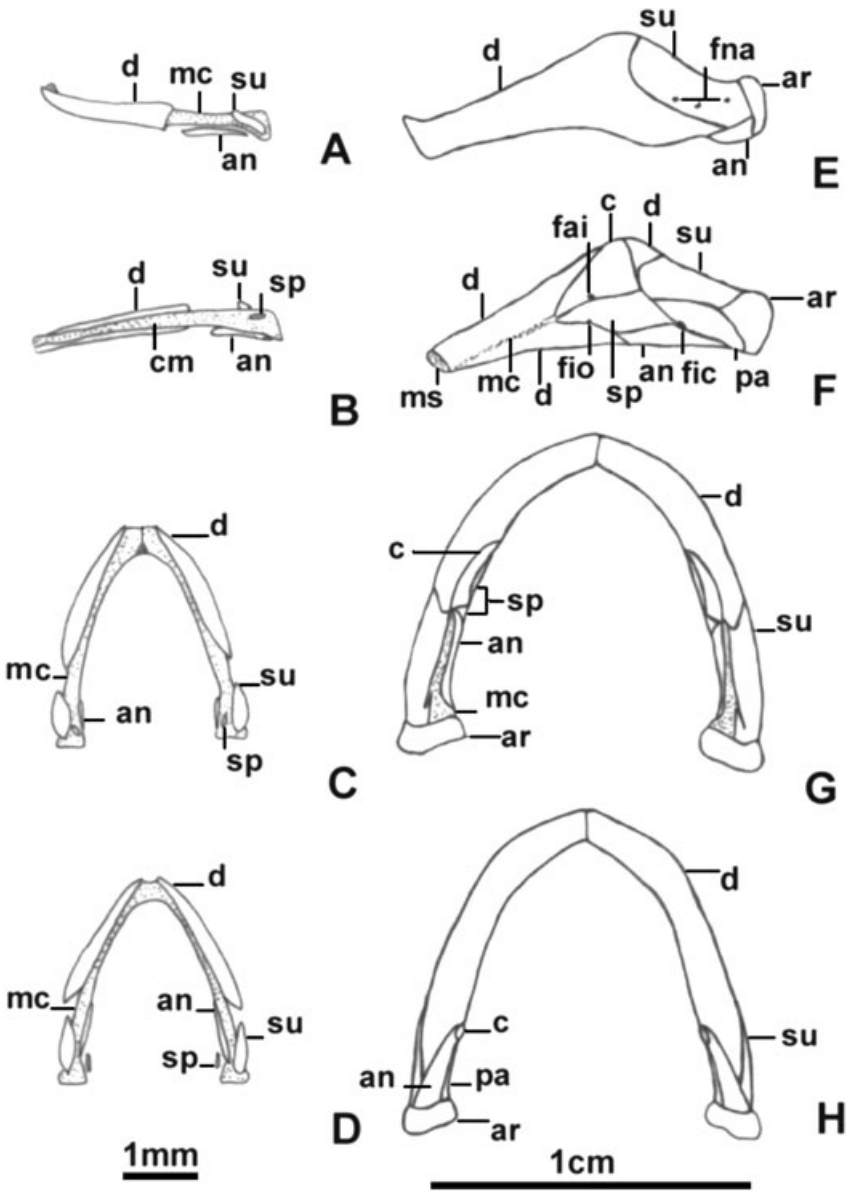

Fig. 2—Meckel's cartilage and mandibular bones of *Phrynops hilarii*. —**A**. Lateral, —**B**. medial, —**C**. dorsal, and —**D**. ventral views of a stage 19 embryo (MLP R. 5321). —**E**. Lateral, —**F**. medial, —**G**. dorsal, and —**H**. ventral views of an adult male (FML 14953). Abbreviations: an, angular; ar, articular; c, coronoid; d, dentary; fai, foramen alveolare inferius; fic, foramen intermandibularis caudalis; fio, foramen intermandibularis oralis; fna, foramina nervi auriculari; mc, Meckel's cartilage; ms, mandibular symphysis; pa, prearticular; sp, splenial; su, surangular.

to the otic capsule. It is slightly longer than the capsule and approximately the same height in lateral view. This cartilage is laterally and ventrally open at the anterior region forming the cavum tympani (Fig. 1B,C). The quadrate cartilage bears the articular surface for the mandible. The medial tip of the quadrate cartilage projects anteriorly as pterygoquadrate cartilage (Fig. 1B,C). At this and in subsequent stages the pterygoquadrate cartilage lacks an ascending process (Fig. 1B,C). The cartilaginous columella is formed by a rod-like portion that traverses obliquely the space between the fenestra ovalis of the otic capsule and the lateral opening of the cavum tympani (Fig. 1B,C). This rod enters the cavum tympani ventrally. In the area of contact with the lateral opening of the cavum the columella is 'pea'-shaped expanded and presents a well-developed ventral process.

Meckel's cartilage. Meckel's cartilages are well chondrified at the first available stage (stage 19; Fig. 2A–D). They converge cranially towards the midline where they form the cartilaginous symphysis and present a stout, triangular dorsal protuberance. At stage 23 all the dermal bones of the mandible are formed and Meckel's cartilage is more reduced but also present. From this stage to adults there is a progressive increment of the bone areas and a reduction of cartilage. However, in subadults and adults some cartilage remains between the fully formed bones of the mandible (Fig. 2E–H).

Hyoid apparatus. The corpus hyoidis is well chondrified at stage 19 (Fig. 3A). Their free anterior ends are open and partially encircling the glottis. The posterior portion of the corpus hyoidis shows a deep dorsal axial area into which

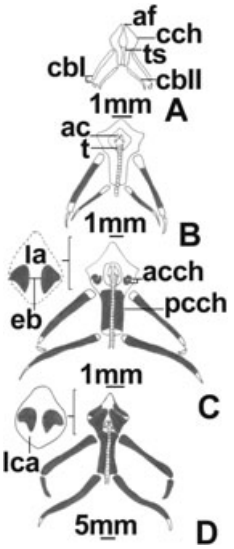

Fig. 3—Ventral views of the hyoid apparatus of *Phrynops hilarii*. —**A**. Stage 19 (MLP R. 5321), —**B**. stage 23 (MLP R. 5324), —**C**. stage 26 (MLP R. 5331), —**D**. subadult male (MLP R. 5337). Black areas indicate bone, white areas are cartilage. Abbreviations: ac, arytenoid cartilages (glottis); acch, anterior centres of the corpus hyoidis; af, anterior fissure; cbI, cornu branchialium I; cbII, cornu branchialium II; cch, corpus hyoidis; eb, entoglossal bones; la, lingual anlage; lca, lingual cartilage; pcch, posterior centre of the corpus hyoidis; t, trachea; ts, tracheal sulcus.

extends the trachea. At stage 22 the adult shape of the corpus hyoidis appears (see Fig. 3B for a stage 23 corpus hyoidis). The anterior ends come into contact, encircling the glottis completely, and project forward forming the lingual process. The left and right cornua branchialia I are well chondrified at stage 19 (Fig. 3A). Each one possesses two bars of cartilage. One of them is longer and proximal and articulates with the anterolateral face of the corpus hyoidis. The other is medially curved and articulates with the first segment. The left and right cornua branchialia II are well chondrified. They are formed by only one bar of cartilage slightly smaller than the first segment of the cornu branchialium I. It articulates proximally with the most posterior end of the corpus hyoidis.

Osteocranium – neurocranium

Supraoccipital. The unpaired supraoccipital ossifies endochondrally at stage 23 through an unpaired centre located in the tectum synoticum (Fig. 4C,I; Table 1). The supraoccipital contacts the exoccipitals and partially overlaps the parietals. The posterior margin of the supraoccipital is slightly concave in dorsal view. The supraoccipital closes the foramen magnum dorsally during all stages of the embryo's development, while in adults the supraoccipital is excluded from the foramen magnum by the exoccipitals. At stage 26 the supraoccipital is sutured to exoccipitals and parietals. The posterior margin of the supraoccipital may be straight or a dorsal crista supraoccipitalis may be already insinuated in more advanced specimens (MLP R. 5332). Adult morphology is attained through bone remodelling and redeposition, which occur mainly along the midline. In subadults and adults the supraoccipital is located on the dorsal midline forming the posterior half of the cranial vault (Fig. 5A,E). The supraoccipital is sutured to parietals, epiotics, prootics, opisthotics and exoccipitals. The supraoccipital is excluded from the foramen magnum by the exoccipitals contacting at the midline. The short crista supraoccipitalis does not project beyond the level of the occipital condyle.

Exoccipital. The paired exoccipitals ossify endochondrally at stage 21 on the lateral sides of the occipital arch (Table 1). At stage 22 exoccipitals are already well ossified but not contacting other bones (Fig. 4E). Each exoccipital forms three ventral pillars that partially circumscribe the two foramina for the hypoglossus nerve. At stage 23 the exoccipitals overlap the supraoccipital (Fig. 4C,F). The contact with the basioccipital is evident at stage 26 at the anterior and middle pillars. The anterior foramen for the hypoglossus nerve is therefore well delimited whereas the posterior foramen remains open caudally. The processes formed by the exoccipital at the base of the occipital condyle are only noticeable at stage 26, although the condyle is still cartilaginous. From this stage on, the suture between exoccipital, supraoccipital and opisthotic becomes visible. In subadults and adults both exoccipitals surround the foramen magnum, form part of the occipital condyle and are sutured to supraoccipital, opisthotics and basioccipital (Fig. 5E).

Basioccipital. The unpaired basioccipital ossifies endochondrally at stage 22 from a single centre located in the basal plate (Fig. 4E; Table 1). At this stage it does not contact other ossification centres. In less advanced stage 23 specimens a ventral centre is added to the pre-existent one (MLP R. 5326). This new chondral centre is shaped like a horseshoe opening to the rear. In more advanced specimens of this stage (MLP R. 5324–5) both centres unite (Fig. 4F) so the basioccipital ossifies in two portions: one infrachordal and one suprachordal. In more advanced specimens at stage 26 (MLP R. 5331) the basioccipital contacts the exoccipitals, but the occipital condyle is still cartilaginous. In subadults and adults the basioccipital constitutes the ventral portion of the occipital condyle with subtriangular outline in ventral view (Fig. 5B,E). It is sutured to exoccipitals, opisthotics and parabasisphenoid.

Basisphenoid and parasphenoid (parabasisphenoid). The single endochondral ossification centre of the basisphenoid appears at stage 21 at the anterior level of the parachordals, crista sellaris and posterior trabecular portion (Table 1). The two

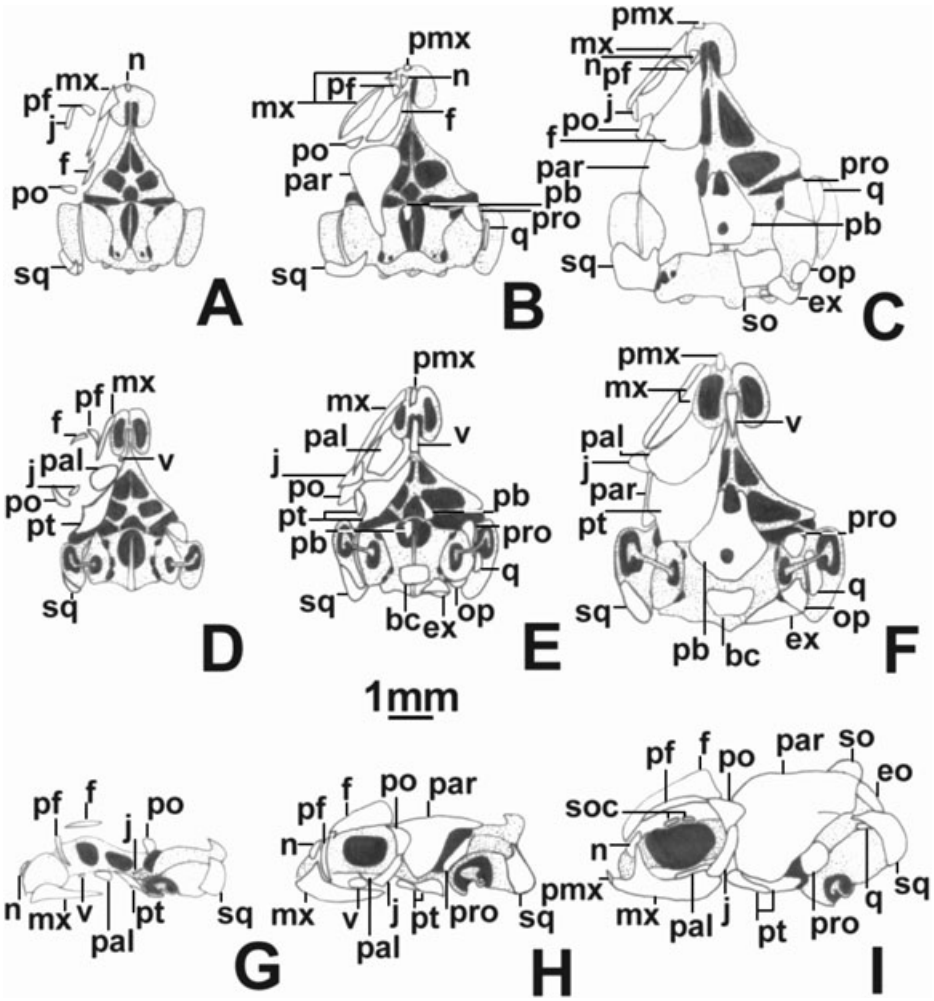

Fig. 4—Osteocranium of *Phrynops hilarii*. —**A**, **D**, **G**. Stage 19 (MLP R. 5321); —**B**, **E**, **H**. stage 22 (MLP R. 5323) and —**C**, **F**, **I**. stage 23 (MLP R. 5324). —**A**–**C**. Dorsal, —**D**–**F**. ventral, and —**G**–**I**. lateral views. Black areas represent cranial foramina and openings. Stippled areas are cartilage, white areas are bone. In dorsal and ventral views, dermal bones were not illustrated on the right side. Abbreviations: bc, basioccipital; eo, epiotic; ex, exoccipital; f, frontal; j, jugal; mx, maxilla; n, nasal; oc, scleral ossicles; op, opisthotic; pal, palatine; par, parietal; pb, parabasisphenoid; pf, prefrontal; pmx, premaxilla; po, postorbital; pro, prootic; pt, pterygoid; q, quadrate; so, supraoccipital; sq, squamosal; v, vomer.

dermal centres of the parasphenoid appear at stage 22 at the level of the membranous floor that closes the pituitary and basicranial fenestrae (Fig. 4B,E). Both parasphenoid centres occur in the same plane as the ossification of adjacent cartilages (parachordal cartilages, trabeculae, and crista sellaris). At stage 23 the trabecular part of the parabasisphenoid overlaps the pterygoid dorsally (Fig. 4C,F). In the more advanced specimen of this stage (MLP R. 5325) both pituitary and basicranial fenestrae are closed by the dermal centres of the parabasisphenoid. At this stage this bone becomes sutured to the pterygoids and overlaps the prootics. In subadults and adults the parabasisphenoid is an unpaired medial bone forming the floor of the cephalic cavity anterior to the basioccipital (Fig. 5B). The parabasisphenoid bears a short sphenoidal rostrum (the ossified intertrabecular plane) and sutures the pterygoids, prootics and basioccipital.

Epiotic. Each paired epiotic ossifies perichondrally in advanced stage 23 specimens at the posterodorsal wall of the otic capsule (Fig. 4I; Table 1). The centres of both epiotics are ventral to the lateral margin of the supraoccipital, which they almost contact. At stage 26 they do not contact the remaining periotic bones yet but are already fused to the supraoccipital. In subadults and adults the epiotics are indistinguishable from the supraoccipital and are sutured to prootics and opisthotics (Fig. 5C,E).

Table 1 Ossification sequence of *Phrynops hilarii*

	Skull	Carapace and vertebral column	Pectoral girdle and forelimb	Pelvic girdle and hindlimb
19	Maxilla	Epiplastra	**Humerus**	**Femur**
	Pterygoid	Entoplastron	**Radius**	**Tibia**
	Palatine	Hyoplastra	**Ulna**	**Fibula**
	Squamosal	Hipoplastra		
	Postorbital	Xiphiplastra		
	Prefrontal			
	Jugal			
	Nasal			
	Vomer			
	Dentary			
	Surangular			
	Angular			
	Splenial			
	Frontal			
21	Parietal	**VC CeV II–VIII**	**Scapula**	**Ilium**
	Premaxilla	**VC DV I–II**	Interclavicle	**Ischium**
	Columella	**Dorsal ribs II–V**		**Pubis**
	Basisphenoid			**MTs I and IV**
	Exoccipital			
	Cornu branchialium I (proximal)			
22	**Prootic**	**Dorsal ribs VI–IX**	**Precoracoid**	**MTs II and III**
	Opisthotic	Costals I–VIII	**Metacoracoid**	
	Basioccipital	**NA CeV I–VIII**	**MCs II–IV**	
	Parasphenoid	**VC DV III–X**		
	Quadrate	**Sacral vertebrae**		
	Coronoid	**VC CaV I–V**		
	Prearticular	**NAs CaV I–VIII**		
	Cornu branchialium II			
23	**Supraoccipital**	**Dorsal rib I**	**MCs I and V**	**1° PH D I, III–V**
	Epiotic	**Atlantic centrum**	**All PHs**	**2° PH D I–V**
	Anterior corpus hyoidis	**NA DV I–X**		**3° PH D II–V**
	Scleral ossicles	**VC CaV VI–XIV**		
	Stapedial footplate	**NAs CaV IX–XVII**		
		Neurals III–VIII		
		Nucal		
25		**VC CaV XV–XX**		
		Neural II		
26	**Articular**	**CaV XIX–XX**	**Intermedium**	**MT V**
	Entoglossal bones	Neural IX	**Ulnare**	**1° PH D II**
	Posterior corpus hyoidis			**4° PH D V**
PH	**Cornu branchialium I (distal)**	**Atlantic intercentrum**	**Centrals**	**Basipodium**
			Distals	**5° PH D V**
	Medial process of the jugal	**Dorsal rib X**	**Prepollex**	
		Sacral ribs	**Pisiform**	
		Peripherals		
		Suprapygal		

Chondral bones are given in bold type.
Abbreviations: CaVs, caudal vertebrae; CeVs, cervical vertebrae; D, digits; DVs, dorsal vertebrae; MCs, metacarpals; MTs, metatarsals; NA, neural arch; PHs, phalanges; VC, vertebral centra.

Prootic. The paired prootics ossify perichondrally at stage 22 on the anterolateral wall of the otic capsule (Fig. 4B,E,H; Table 1). In a stage 25 specimen, the prootics contact the quadrates and the posterior margin of the descending portion of the parietals (MLP R. 5330). Prootics and quadrates become sutured at stage 26 forming the stapediotemporal foramen. The trigeminal nerve foramen is delimited by prootics and parietals. In subadults and adults the prootics

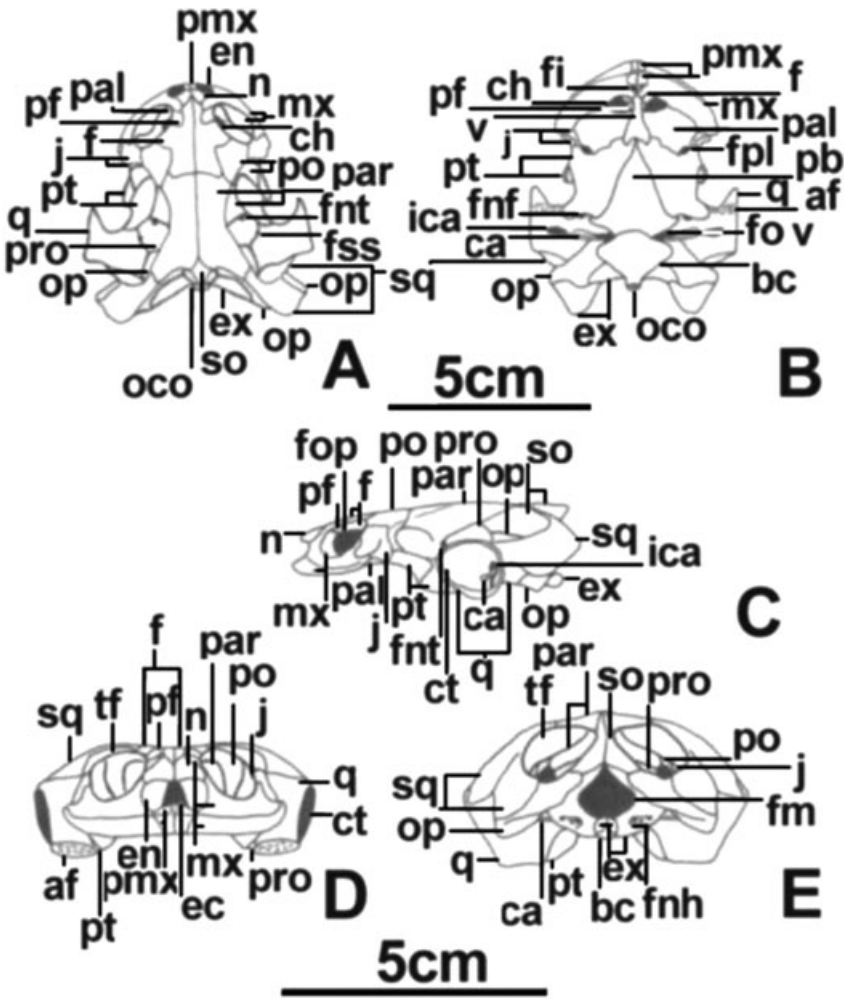

Fig. 5—Adult osteocranium of an adult male of *Phrynops hilarii* (FML 14953). —**A**. Dorsal, —**B**. ventral, —**C**. lateral, —**D**. anterior, and —**E**. posterior views. Black areas represent cranial foramina and openings. Abbreviations: af, articular face of the quadrate; ca, columella; ch, choana; ct, cavum tympani; ec, encephalic cavity (view in part through the nares and in part through the orbitonasal foramen); en, external naris; fi, foramen intermaxillaris; fm, foramen magnum; fnf, foramen nervi facialis; fnh, foramina nervi hypoglossi; fnt, foramen nervi trigemini; fop, foramen opticum; fov, fenestra ovalis; fpl, foramen palatinum posterius; fss, foramen stapedio-temporale superius; ica, incisura columella auris; oco, occipital condyle; tf, temporal fossa. Other abbreviations as in Fig. 4.

are part of the anterior half of the floor of the temporal fossa (Fig. 5A,C). They are sutured to parietals, epiotics, quadrates and opisthotics.

Opisthotic. The paired opisthotics ossify perichondrally at stage 22 at the posterior wall of the otic capsule (Fig. 4E; Table 1). At stage 23 the opisthotics contact the quadrate (Fig. 4C,F) and at stage 26 they become sutured to exoccipitals, quadrates and squamosals. In subadults and adults the opisthotics form the posterior floor of the temporal cavity and together with the exoccipitals form the paroccipital processes (Fig. 5A,C,E). The opisthotics are sutured to quadrates, squamosals, prootics, epiotics, exoccipitals, basioccipital and exoccipitals.

Scleral ossicles. The scleral ossicles begin to ossify dermally within the sclera at stage 23 (Fig. 4I, Table 1). The following features were observed: (1) ossification begins in the dorsal ossicles of the ring and progresses ventrally; (2) the number of ossified ossicles in each specimen is not always bilaterally symmetrical; (3) the ring of ossicles is always open ventrally; (4) the largest ossicles are always the three elements situated on the dorsal part of the ring; and (5) the ossicles are not imbricated. In the more advanced specimen of stage 26 (MLP R. 5332) the sclerotic ring is completely defined. In this specimen the ring is formed by 13 (right side) or 14 (left side) ossicles. The ventralmost ossicle on the left side is small and does not participate in the external (lateral) margin of the ring. We could not observe the scleral ossicles of the subadults and adults because they were lost during the preparation of the material.

Osteocranium – splachnocranium

Quadrate. The quadrate ossifies endochondrally at stage 22 at the anterior and medial half of the quadrate cartilage (Fig. 4B,E; Table 1). At stage 23 the quadrate occupies the anterior roof of the cavum tympani (Fig. 4C,F,I). At stage 26

the completely ossified quadrate contacts the pterygoid and is sutured to squamosal and prootic. In subadults and adults the quadrate is sutured to prootic, opisthotic, squamosal, pterygoid and parabasisphenoid (Fig. 5A–E). The quadrate extends laterally over the fossa temporalis superior delimiting the conical cavum tympani. This cavum has a suboval opening where the tympanic membrane rests. The antrum postoticum is almost delimited anteriorly by the quadrate and posteriorly by the squamosal. The quadrate forms the articular fossa for the lower jaw together with the pterygoid.

Epipterygoid. The ascending process of the palatoquadrate is absent in all specimens examined.

Articular. The articular ossifies endochondrally at stage 26 (Table 1) occupying the caudalmost end of the Meckel's cartilage. In subadults and adults the articular occupies the posterior tip of the mandible, forms the articular condyle and is sutured to angular, splenial and surangular bones (Fig. 2E–H). In a medial view the articular forms the ventral margin of the fossa meckelii.

Columella auris. The columella ossifies perichondrally at stage 21 (Table 1). In some stage 23 specimens, the stapedial footplate ossifies as a dilated new laminar chondral ossification. Both centres contact each other at stage 26, although the distal end remains cartilaginous.

In subadults and adults the columella is a completely ossified thin rod located in the cavum acustico-jugulare and is slightly expanded distally so that it appears conical in lateral view (Fig. 5B,C,E). The stapedial footplate is shaped like a disk.

Corpus hyoidis. The corpus hyoidis ossifies perichondrally in some stage 23 specimens (Table 1). The paired elongated centres are placed at both sides of the tracheal sulcus. In advanced stage 25 specimens (MLP R. 5330) these centres fuse to each other. Each hyoid process ossifies perichondrally at stage 26 in the laterals of the opening for the glottis (Fig. 3C).

In subadults and adults the corpus hyoidis is longer than wide (Fig. 3D). Its anterior third is triangular and perforated by the opening for the glottis. This opening is flanked by the completely ossified hyoid processes and ends in a short cartilaginous lingual process. The posterior portion of the corpus hyoidis occupies two-thirds of its total length, bears a dorsal tracheal sulcus for passage of the trachea, and articular facets for the cornua branchialia I and II.

Cornu branchialium I. The cornu branchialium I ossifies perichondrally at stage 21 (Table 1). At stage 26 this segment is almost completely ossified but both its ends are still cartilaginous (Fig. 3C). The distal segment ossifies after hatching. In subadults and adults both segments are completely ossified and maintain the same proportions and topographical relationships as described for embryos (Fig. 3D). The distal end of the first segment and the entire second one are embedded in the cervical musculature.

Cornu branchialium II. The cornu branchialium II ossifies perichondrally at stage 22 (Table 1). At stage 26 it is almost completely ossified except for its proximal and distal ends (Fig. 3C). In subadults and adults the almost completely ossified cornu branchialium II is thinner than the first cornu and is embedded in the cervical musculature (Fig. 3D).

Osteocranium – dermatocranium

Nasal. The paired nasals ossify dermally at stage 19 as drop-shaped elements on the anterior wall of each nasal capsule and dorsal to the external nares (Fig. 4A,G; Table 1). Nasals develop to attain the characteristic triangular outline seen in adults. At stage 23 they contact the prefrontal and frontal (Fig. 4C,I) and at stage 26 become sutured to them and to the prefrontal process of the maxilla. At this stage the nasals do not contact each other on the midline. In subadults and adults nasals are small triangular elements forming the posterior margins of the external nares (Fig. 5A,D). Both nasals are sutured to each other anteriorly, whereas they are separated caudally by the frontals. Nasals are sutured to maxillae, premaxillae and frontals.

Prefrontal. The paired prefrontals ossify dermally at stage 19 on the anterodorsal region of the circumorbital ring (Fig. 4-A,D,G; Table 1). At stage 21 the prefrontals overlap the frontals. At stage 23 the frontals contact the nasals (Fig. 4C,I). Frontals become sutured to nasals, frontals and maxillae at stage 26. In subadults and adults prefrontals are small bones placed on the anteromedial margin of the orbits. They suture to frontals, nasals and maxillae (Fig. 5A,C,D).

Frontal. The paired frontals ossify dermally at stage 19 on the dorsal portion of the circumorbital ring, overlapping the prefrontals, postorbitals and parietals (Fig. 4A,D,G; Table 1). At stage 23, frontals overlap the nasals and contact each other only in the more advanced specimen (Fig. 4C,I). At stage 26 frontals are sutured to each other (this condition varies among the specimens examined) and to adjacent bones (prefrontals, parietals, postorbitals and nasals). In subadults and adults the frontals show a slight anterolateral projection that reaches the posteromedial edge of the orbits. Frontals are sutured to postorbitals, maxillae, nasals, prefrontals and parietals (Fig. 5-A,C,D).

Parietal. The paired parietals ossify dermally at stage 21 posterior to the circumorbital ring at the vault level. They overlap frontals and postorbitals and extend above the otic capsule (Table 1). At stage 22 parietals grow ventrally until almost contacting the pterygoids (Fig. 4B,H). At stage 23 parietals overlap the squamosals and the supraoccipital and

begin to contact each other in their posterior medial margins (Fig. 4C,F,I). In one stage 25 specimen (MLP R. 5328) both parietals contact each other along the entire length. At stage 26 the parietals become sutured to prootics, pterygoids, postorbitals, frontals, supraoccipital and squamosals.

At this stage the middle union between both parietals is by localized sutures. In some specimens (MLP R. 5331) parietals remain separated anteriorly delimiting together with the frontals a large irregular frontoparietal fontanelle. Other specimens show almost complete suture between parietals so that the fontanelle is reduced (MLP R. 5336) or obliterated (MLP R. 5334–5335). In subadults and adults parietals extend dorsally and ventrolaterally to form most of the roof and anterolateral walls of the cephalic cavity (Fig. 5A,C,E). In dorsal view it presents an hourglass-shaped outline because of the marked lateral emargination of the skull. The posterior margins of the parietals are notched because of the presence of occipital emarginations. Parietals are sutured to each other along the entire midline except at the posteriormost region where they are slightly separated by an anterior projection of the supraoccipital. Parietals are sutured to frontals, postorbitals, pterygoids, prootics and supraoccipitals.

Postorbital. The paired postorbitals ossify at stage 19 dorsal to the jugal on the posterior region of the circumorbital ring (Fig. 4A,D,G; Table 1). At stage 21 the postorbitals overlap the jugals, frontals and parietals, with which they become sutured at stage 26. At stage 26 postorbitals contact the pterygoids at the level of the trochlear process.

In subadults and adults postorbitals form the posterior medial half of orbit and are sutured to frontals, parietals, jugals and pterygoids (Fig. 5A,C).

Squamosal. The paired squamosals ossify dermally at stage 19 dorsally to the posterolateral region of the quadrate cartilage (Table 1; Fig. 4A,D,G). Squamosals bear the squama (closely overlying the quadrate) and the spine (dorsal process). At stage 23 the spine contacts the parietal (Fig. 4C,F,I). At stage 26 squamosals become sutured to parietals and quadrates. Squamosals and quadrates form the cavum tympani. In subadults and adults the squamosal spines and the parietals form the thin temporal bars (Fig. 5A,C). The squamosal squama and the quadrate form the posterior wall of the cavum tympani and of the antrum postoticum. The squamosals form paroccipital processes together with opisthotics.

Premaxilla. The paired premaxillae ossify dermally at stage 21 (Table 1). From this stage on, both labial ridge and dorsal laminar process are present. The latter covers the nasal capsule anteriorly, below the external nares. At stage 22 the premaxilla grows posteriorly at palatal level to form the anterior margin of the choana (Fig. 4B,E) and at stage 23 it contacts the maxilla (Fig. 4C,F,I). At stage 26 the premaxillae are still not sutured at midline and contact the vomer. The posterior margin of each premaxilla bears a notch. This notch is closed by the medial expansion of the maxilla that excludes the premaxilla from the choana. In subadults and adults both small premaxillae are sutured to each other forming the anteriormost tip of the upper jaw, as well as part of the ventromedial margin of the external nares (Fig. 5A,B,D). Both premaxillae are sutured to the maxillae forming the labial ridge.

Maxilla. Each maxilla ossifies dermally at stage 19 occupying the entire margin of the upper jaw lateral to the nasal capsule and the palatine (Fig. 4A,D,G; Table 1). Each maxilla has a dorsal process (= prefrontal process) and a labial ridge. The dorsal process is triangular and anterior overlying the nasal capsule. The labial ridge extends along the entire length of the maxilla. In turn, each maxilla extends medially onto the horizontal plane of the palate. At stage 21 the prefrontal process contacts widely to prefrontal, whereas the maxilla overlaps the jugal and palatine. At stage 26 the maxilla issues two laminar anteroventral processes that delimit the choana together with the palatine and vomer. At this same stage the maxilla becomes sutured to palatine, premaxilla, prefrontal and jugal. In subadults and adults the maxilla forms most of the external arch of the upper jaw and is sutured to prefrontal and nasal through the prefrontal process. This process delimits partially the external naris and the orbit (Fig. 5A–D). The maxilla extends posteriorly forming the ventral margin of the orbit and reaching the jugal. The maxilla and the premaxilla form the triturating surface of the upper jaw and the 'cutting' labial ridge. Both maxillae contact each other on the midline forming the anterolateral margin of the choana.

Jugal. The paired jugals ossify dermally at stage 19 in the posteroventral region of the circumorbital ring (Fig. 4A,D,G; Table 1). At stage 21 they become sutured to pterygoids, maxillae and postorbitals. At stage 23 the jugals contact the palatines (Fig. 4F).

In subadults and adults jugals delimit the posteroventral margins of the orbits and are sutured to maxillae, postorbitals and palatines (Fig. 5A–E). In adults there is a small bone visible in a ventral view between the pterygoid, palatine, maxilla and jugal. This small bone seems to represent the medial process of the jugal (Fig. 5B). The separate medial process of the jugal appears during posthatching ontogeny.

Osteocranium – palatal bones

Vomer. The small, paired vomers ossify at stage 19 between the pterygoids and the foramina prepalatina (Fig. 4D,G, Table 1). At stage 21 both vomers are considerably larger, contacting each other on the midline and the maxillae laterosposteriorly. At stage 22 both vomers fuse to each other and become fusiform anteriorly (Fig. 4E,H). At stage 23 the vomer is partially hidden because of extensive anteromedial

development of the pterygoids (Fig. 4F). At stage 26 the anterior end of the vomer becomes dilated ending as a flat margin at the point of contact with the premaxillae. At this stage the vomer sutures to palatines and pterygoids. In subadults and adults the unpaired vomer is expanded laterally at its anterior and posterior portions forming the medial margin of each choana together to the palatines (Fig. 5B). The vomer sutures to maxilla, palatines and pterygoids.

Palatine. The paired palatines ossify dermally at stage 19 (Table 1; Fig. 4D,G). At stage 21 palatines contact the maxillae, pterygoids and vomers. At this stage palatines, maxillae, premaxillae and vomers delimit a palatal fenestra occupied by the cartilaginous floor of the nasal capsules, bearing the opening of the choana. At stage 23 the palatines contact the jugal (Fig. 4F,I). At stage 26 the palatines become sutured to pterygoids and maxillae, and in some individuals (MLP R. 5335) also to the vomer. In subadults and adults the palatines extend along the anterior section of the palate, delimiting the choana posteriorly (Fig. 5B). The palatines are sutured to pterygoids, vomer and maxillae. The small foramen palatinum posterius opens between palatines and pterygoids.

Pterygoid. The paired pterygoids ossify dermally at stage 19 (Table 1). The axially elongated pterygoids lay ventral to the pterygoquadrate cartilages and lateral to trabeculae and parachordals (Fig. 4D,G). At stage 19 the pterygoids represent two-thirds of the neurocranial length. Halfway along their length there are a lateral triangular expansion (= transverse flange) directed toward the jugal. The transverse flange divides the pterygoid into two arms: the anterior arm (medial to palatine) and the posterior arm (= quadrate arm). At stage 21 the quadrate arm is nearer to the quadrate cartilage. The transverse flange contacts the jugal and its posterior margin shows the adult shape of the trochlear process. Although the trochlear process of the pterygoids is a feature unique of the Pleurodira, its development is not gradual, instead it shows the same shape as the adults since stage 21. At stage 22 the quadrate arm grows until it almost contacts the descending process of the parietal (Fig. 4E,H). At this stage the pterygoids overlap the palatines and vomer. At stage 23 the pterygoids cover ventrally the 'trabecular' portion of the parabasisphenoid (Fig. 4F,I). At stage 26 the pterygoids become sutured to palatines, vomer and jugals. In subadults and adults the pterygoids are the largest of the palatal bones (Fig. 5B). Both pterygoids are sutured each other anteriorly but are posteriorly separated by the parabasisphenoid. The pterygoids are sutured to palatines, vomer, postorbitals, squamosals, prootics and parietals. The pterygoids participate in the following structures: (1) anterior region of the articular surface for the mandible; (2) anterior margin of the foramen posterius canalis carotici interni together with the quadrate; (3) medial margin of the laterally open subtemporal fenestra; and (4) trochlear process.

Osteocranium – dermal bones of the mandible

Dentary. The dentary ossifies dermally at stage 19 (Table 1). It is placed on the anterolateral half of Meckel's cartilage occupying two-thirds of the latter and being the largest centre of the mandible (Fig. 2A–D). At stage 22 the dentary articulates with the adjacent bones and bears the labial ridge and the lingual margin of the mandible. In subadults and adults the dentary occupies four-fifths of the external mandibular surface and is fused to coronoid, prearticular, surangular and splenial bones (Fig. 2E–H). Both dentaries are sutured at the symphysis and present a cutting labial ridge along the anterior half of the lower jaw. The labial margin of the triturating mandibular surface is more developed than its lingual margin. The dentary delimits the sulcus cartilaginis meckelii, which extends along the anterior part of the mandible.

Angular. The angular ossifies dermally at stage 19 (Table 1). The angular is similar to the surangular in length but smaller than the latter in area (Fig. 2A,D). At stage 22 the angular articulates with the adjacent bones. In subadults and adults the elongated angular occupies approximately one-third of the length of the lower jaw (Fig. 2E–H). The angular is sutured to all the bones of the mandible.

Splenial. The splenial ossifies dermally at stage19 (Fig. 2B–D; Table 1) by a small centre dorsal to the angular. The splenial articulates with the adjacent bones since stage 22. In subadults and adults the splenial occupies the central sector of the internal side of each hemimandible (Fig. 2F–G). The splenial is sutured to all dermal bones of the mandible and delimits part of the sulcus cartilaginis meckelii and part of the fossa meckelii.

Coronoid. The coronoid ossifies dermally at stage 22 (Table 1). It is placed on the lingual side of the Meckel's cartilage, and contacts the dentary and splenial. In subadults and adults the coronoid is a small subtriangular bone placed at the posterior and dorsal half of the mandible forming the coronoid process together with the dentary (Fig. 2F–H). It is sutured to surangular, dentary and splenial.

Surangular. The surangular ossifies dermally at stage 19 and lays dorsally on the posterolateral third of the Meckel's cartilage (Fig. 2A–D; Table 1). The surangular contacts the adjacent bones at stage 22. In subadults and adults the surangular forms the lateral wall of the fossa meckelii, and is sutured to all the bones of the mandible (Fig. 2E–H).

Prearticular. The prearticular ossifies dermally at stage 22 (Table 1). It appears on the lingual side of Meckel's cartilage contacting the dentary and coronoid. The prearticular is similar to coronoid in length, but thinner. In subadults and adults the prearticular is placed ventral to the surangular in

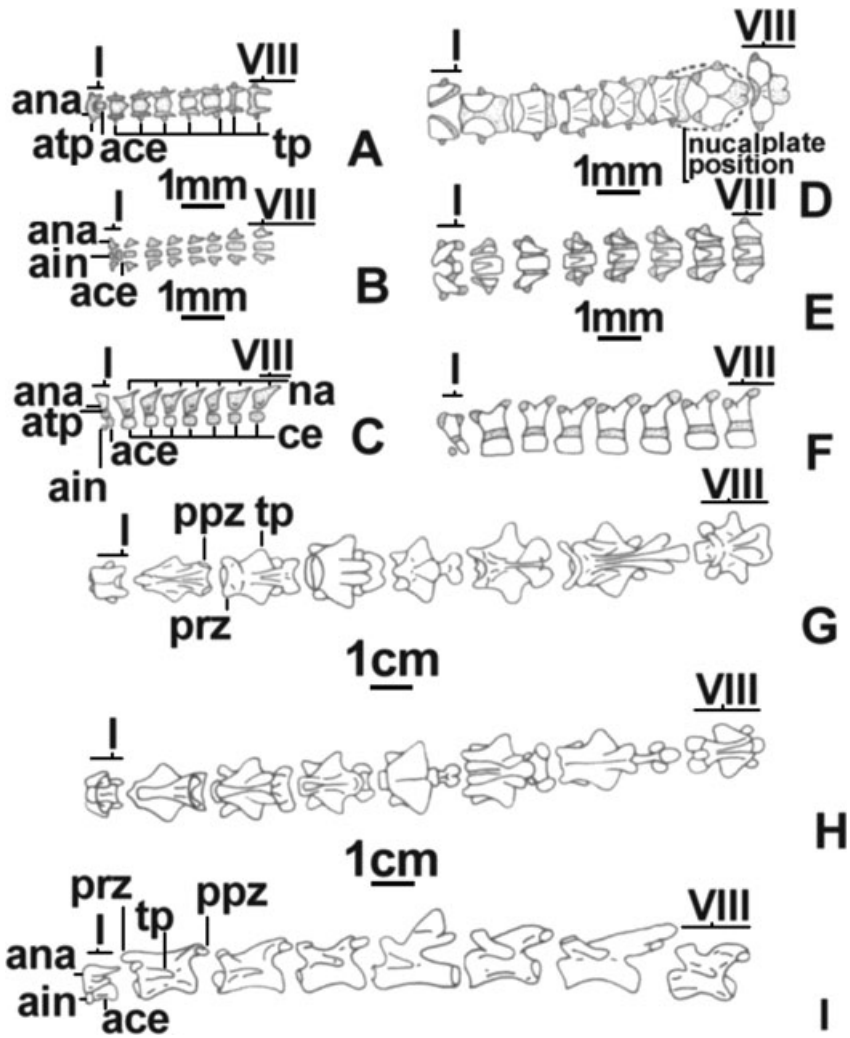

Fig. 6—Cervical vertebrae of *Phrynops hilarii*. —**A**–**C**. Stage 19 (MLP R. 5321), —**D**–**F**. stage 23 (MLP R. 5326), —**G**–**I**. adult (FML 14953). —**A**, **D**, **G**. Dorsal views, —**B**, **E**, **H**. ventral views, —**C**, **F**, **I**. lateral views. White areas represent bone. Stippled areas represent cartilage. Abbreviations: ace, atlantic centrum; ain, atlantic intercentrum; ana, atlantic neural arch; atp, atlantic transverse processes, ce, vertebral centra of cervicals II–VIII; na, neural arches of cervicals II–VIII; ppz, postzygapophysis; prz, prezygapophysis; tp, transverse processes of cervicals II–VIII.

a medial view and forms a suture with the articular, angular, surangular and splenial (Fig. 2F,H).

Osteocranium – hyoid dermal bones

Entoglossal bones. No Alcian Blue-positive entoglossal cartilage was observed at any of the embryo stages analysed. Both entoglossal bones ossify dermally in the lingual anlage at stage 26 dorsally to the corpus hyoidis and the lingual process, before the formation of the entoglossal cartilage (Fig. 3C; Table 1). In subadults and adults the entoglossal cartilage is well developed (Fig. 3D). The left and right entoglossal bones are not fused and maintain their semicircular shape. These bones comprise approximately 50% of the surface area of the entoglossal cartilage.

Vertebrae

At stage 19 (Figs 6A–C, 7A, 8A, 9A and 10A–C) all regions of the vertebral column are present, with eight cervical (CeV), 10 dorsal (DV), one sacral (SV) and 20 caudal (CaV) vertebrae. These vertebrae are represented by cartilaginous neural arches and centra, and show the following characteristics: (1) all the zygapophyses of the CeV articulate to each other; (2) neural arches contact middorsally only in CeVs VII and VIII; (3) there are 18 transverse processes (nine caudals, two sacrals, and eight cervicals); and (4) the atlas is formed by centrum and intercentrum, both cartilaginous. At stage 21 the following changes occur: (1) beginning of chondral ossification of the vertebral centra of CeVs II–VIII and DVs I–II (Table 1); (2) cartilaginous neural arches of DVs VI–X joined middorsally; (3) there are 22 cartilaginous CaVs, the few posteriormost of these formed by vertebral centra only; and (4) zygapophyses of CaVs VI–IX contacting each other. At stage 22 ossification begins perichondrally: (1) the neural arches of all CeVs; (2) the vertebral centra of DVs III–X; (3) the vertebral centra and neural arches of the SVs; (4) the neural arches of CaVs I–VIII; and (5) the vertebral centra of CaVs I–V (Table 1). At stage 23 (Figs 6D–F, 7B, 8B, 9B and 10D–F) the following events occur: (1) ossification of the

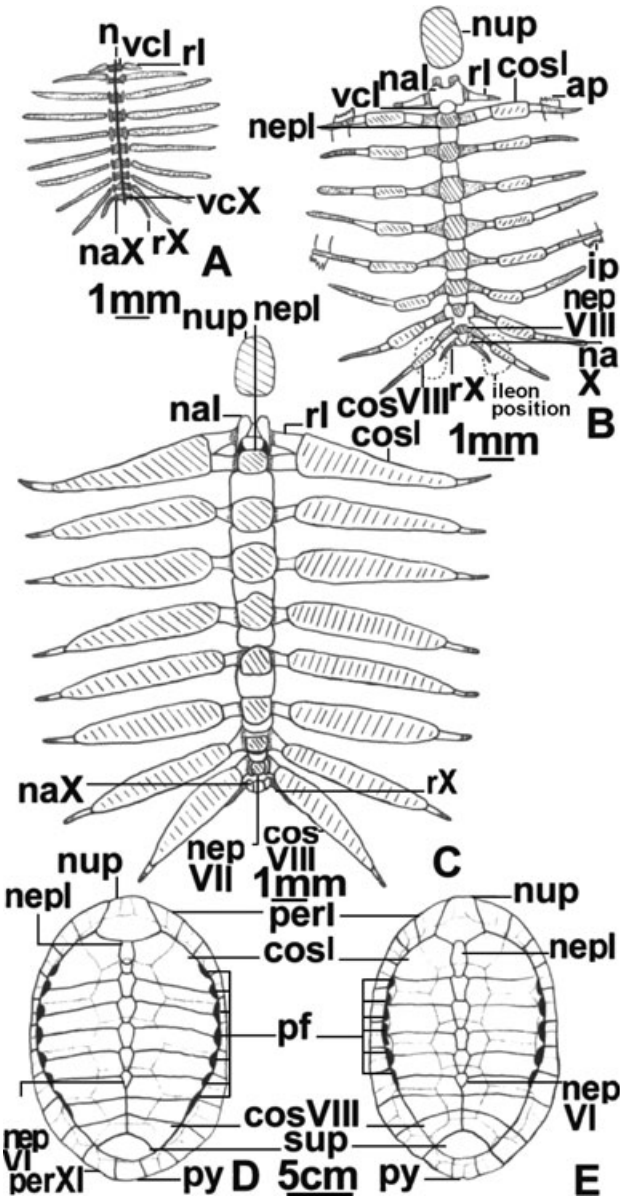

Fig. 7—Dorsal views of the dorsal vertebrae of *Phrynops hilarii* and their associate carapace plates. —**A**. Stage 19 (MLP R. 5321), —**B**. stage 23 (MLP R. 5326), —**C**. stage 26 (MLP R. 5331), —**D**. subadult (MLP R. 5337), and —**E**. adult (MLP Q. 026). —**A**–**C**. White areas represent chondral bone, the dashed areas represent dermal plates, and the stippled areas represent cartilage. —**D**, **E**. Dotted lines represent the sutures between the dermal carapace and the epidermal plates. Abbreviations: ap, axilar pillar; cos I, costal I; cos VIII, costal VIII; ip, inguinal pillar; n, notochord; na I, neural arch dorsal vertebra I; na X, neural arch dorsal vertebra X; nep I, VI, VII, VIII, neural plates I, VI, VII and VIII; nup, nuchal plate; per I, peripheral I; per XI, peripheral XI; pf, peripheral fontanelles; py, pygal; r I, rib I; r X, rib X; sup, suprapygal; vc I, vertebral centrum I; vc X, vertebral centrum X.

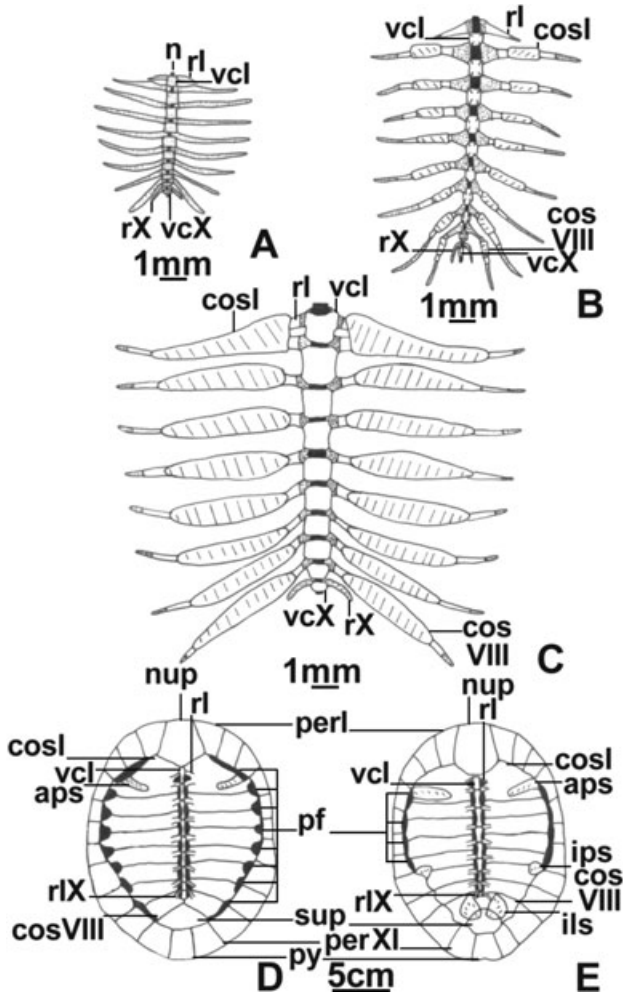

Fig. 8—Ventral views of the dorsal vertebrae of *Phrynops hilarii* and their associate carapace plates. —**A**. Stage 19 (MLP R. 5321), —**B**. stage 23 (MLP R. 5326), —**C**. stage 26 (MLP R. 5331), —**D**. subadult (MLP R. 5337), and —**E**. adult (MLP Q. 026). —**A**–**C**. White areas represent chondral bone, the dashed areas represent dermal plates, and the stippled areas represent cartilage. Abbreviations: aps, axillar pillar suture; ils, ilium suture; ips, inguinal pillar suture; rIX, rib IX. Other abbreviations as in Fig. 7.

atlantic centrum (Table 1); (2) some specimens show osseous contact between vertebral centra and neural arches of all the CeVs; and (3) chondral ossification and middorsal closure of the neural arches of DVs (Table 1). The middorsal closure occurs in anteroposterior direction across regions and within each region with the exception of the atlantic neural arch that never closes middorsally. Also at stage 23 some variability in the number of CaVs (18–20) and the progress of their ossification is observed. These vertebrae begin to ossify at the neural arches in the anteriormost CaVs and at the vertebral centra in the posteriormost ones. At stage 25 the following changes take place: (1) the shape of the

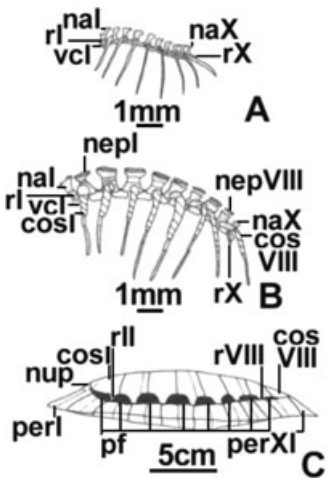

Fig. 9—Lateral views of the dorsal vertebrae of *Phrynops hilarii* and their associate carapace plates. —**A**. Stage 19 (MLP R. 5321), —**B**. stage 23 (MLP R. 5326), and —**C**. subadult (MLP R. 5337). —**A**, **B**. White areas represent chondral bone, the dashed areas represent dermal plates, and the stippled areas represent cartilage. —**C**. Dotted lines represent the sutures between the dermal carapace and the epidermal plates. Abbreviations: rII, rib II. Other abbreviations as in Fig. 7.

articular surface of the CVs begins to attain definition and a biconvex body is clearly distinguished for CeV V; (2) number of CaVs is variable (19–20); and (3) CaVs I–XVII are completely ossified whereas only the centra are ossified in the posteriormost ones. At stage 26 the atlantic intercentrum remains cartilaginous, the adult morphology of the articular facets of the CeVs is defined, and CaVs are completely ossified.

In subadults and adults (Fig. 6G–I) the features of the cervical region are as follows: (1) completely ossified CeVs (including the atlantic intercentrum); (2) atlas (amphicoelous), axis and CeVs III–IV (opisthocoelous), CeVs V and VIII (biconvex), CeV VI (procoelous) and CeV VII (amphicoelous); (3) CeV VII is the longest of the cervical series; (4) CeVs II–VI and VIII are approximately the same length and the atlas is half the length of the axis; (5) all the CeVs present an anterior midventral keel for muscular insertion (absent in the atlas); (6) all CeVs bear well-differentiated and posterolaterally orientated transverse processes; (7) except for the atlas, all the postzygapophyses are placed on a posteromedial projection of the neural arch (peduncle) and their articular facets are well separated and orientated in a slightly oblique plane; (8) the neural arches of CeVs II–VIII are fused middorsally; (9) the axis develops a well-defined neural ridge that projects anteriorly occupying the space between the atlantic postzygaphophyses; and (10) the atlantic body and arches are joined by sutures as well as the atlantic intercentrum and centrum.

The dorsal region of all 'Recent' turtles presents 10 DV; however, the ilium of the Pleurodira is sutured to the carapace mainly at the level of the eighth costal plate. In adult *P. hilarii*, the dorsal ribs of DVs IX and X are incorporated into the eighth costal plate of the dorsal shield, and therefore become involved in the suture with the ilium. This structural design implies that the last two DVs (IX and X) are 'sacralized.' The dorsal region of subadults and adults presents the following characteristics (Figs 7D,E, 8D,E and 9C): (1) amphiplatyan (DVs II–X) or procoelous (DV I) body; (2) DV I with prezygapophyses orientated ventromedially, neural arch sutured to first neural plate, pedicels articulated to the vertebral centrum, and first dorsal rib articulated to the transverse process; (3) DVs II–VIII with vertebral centra compressed, elongated, and decreasing in length toward the rear (DV VIII is shortest and less compressed); (4) neural arches fused to the carapace and anteriorly out of phase with their respective vertebral centra, thus acquiring 'intercentric' position; (5) dorsal ribs 2°–8° also 'intercentric' because they articulate with one neural arch and two successive vertebral centra; (6) vertebral centra and neural arches of all DVs sutured to each other; and (7) vertebral centra of DVs IX and X ('sacralized' vertebrae) short and broad, with the small transverse processes articulated to the proximal tip of dorsal ribs 9° and 10°.

The sacral region of subadults and adults (Fig. 10G–I) presents two SVs with small transverse processes that contact the ilium through a short cartilaginous rib (ossified in adults). The second SV has a posterior condyle that articulates with the anterior cotyle of CaV I.

Length of the caudal region of subadults and adults (Fig. 10G–I) is approximately three-quarters of the length of the dorsal region and comprises 17 procoelous vertebrae, caudally decreasing in thickness and height. This lesser height is the result of the smaller size of the neural arches, with the CaVs I–IV being tallest (neural arches higher than their respective vertebral centra), and CaV XVII shortest (lacking neural arch). In addition, the neural arches of CaVs I–IV present a short neural ridge and a narrow base (two-thirds of the total length of the corresponding vertebral centrum). The transverse processes are present in CaVs I–X, although only those of the first seven CaVs are well developed. The postzygapophyses of CaVs I and III–VII are situated on a peduncle with the posterior margin convex in dorsal view.

Ribs

At stage 19 there are 12 cartilaginous monocipital ribs articulated to the DVs and SVs (Figs 7A, 8A and 9A). The dorsal rib X projects posteriorly, whereas the others project laterally. Both sacral ribs are short with respect to the dorsal ones. At stage 21 the middle region of the dorsal ribs II–V ossifies perichondrally (Table 1). The ossification of the ribs progresses posteriorly to dorsal rib IX at stage 22. At stage 23 the dorsal ribs III–VII bear two additional centres proximally and distally to the middle centre. We are not sure about this peculiarity of the specimen MLP R. 5324 because in all other

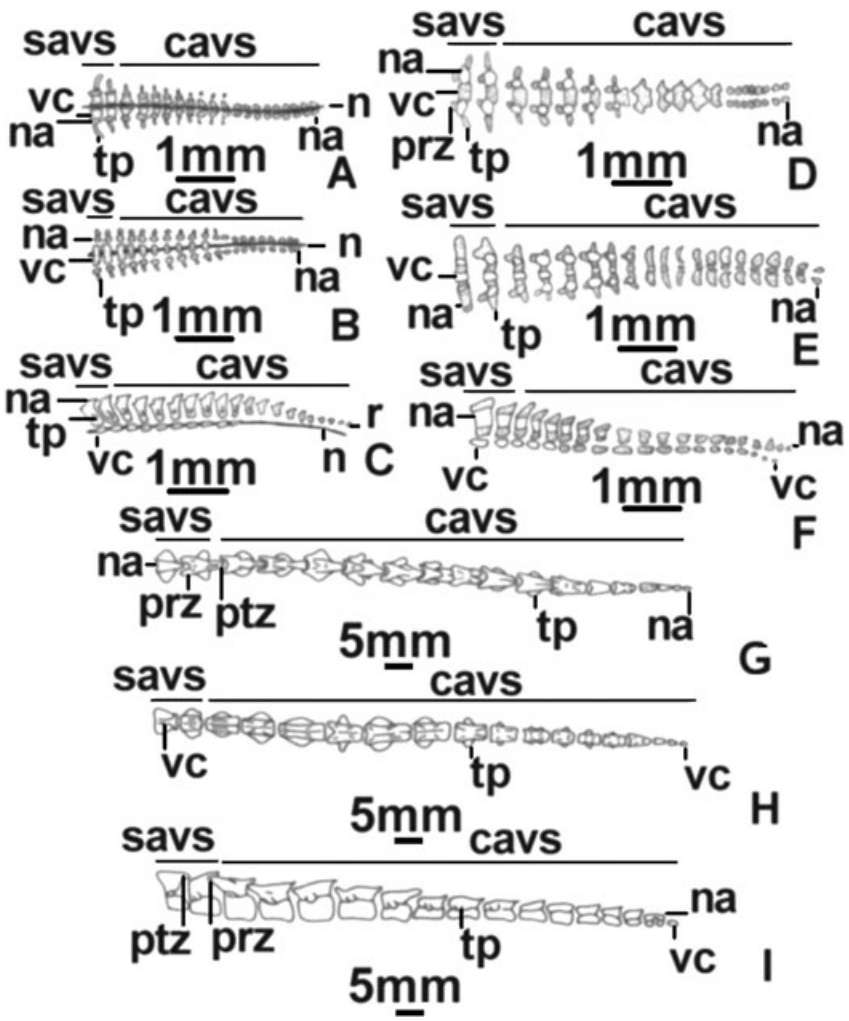

Fig. 10—Sacral and caudal vertebrae of *Phrynops hilarii*. —**A**–**C**. Stage 19 (MLP R. 5321), —**D**–**F**. stage 23 (MLP R. 5326), and —**G**–**I**. adult (MLP Q. 026). —**A**, **D**, **G**. Dorsal views, —**B**, **E**, **H**. ventral views, —**C**, **F**, **I**. lateral views. Abbreviations: cavs, caudal vertebrae; n, notochord; na, neural arch; prz, prezygapophysis; ptz, postzygapophysis; savs, sacral vertebrae; tp, transverse process; vc, vertebral centrum.

stage 23 specimens the dorsal ribs II–IX were almost completely ossified. Dorsal rib I ossifies at stage 23. In subadults there are nine ossified ribs (dorsal ribs I–IX). Dorsal ribs II–IX are incorporated into the costal plates of the carapace and articulate distally with the peripheral plates (Figs 7D,E, 8D,E and 9C). Relative rib length is dorsal ribs III–VI > II and VII > VIII–IX, with dorsal rib I extremely small, approximately one-fifth of the length of dorsal rib II. Dorsal rib I is sutured to the first costal plate anteriorly and to dorsal rib II posteriorly. Orientation of the dorsal ribs varies along the series. Dorsal rib I projects posteriorly. Dorsal rib II is curved, perpendicular to the sagittal axis and incorporated to the first costal plate. Dorsal rib VIII is orientated slightly posteriorly. Dorsal rib IX is markedly caudal and contacts the ilium. The remaining dorsal ribs are perpendicular to the sagittal axis. Both dorsal ribs IX and X and the sacral ribs are thin and circular in transverse section. Instead, the remaining dorsal ribs are broader and flattened. Adults retain the features described for subadults, with the additional ossification of dorsal rib X and sacral ribs.

Carapace

The carapace begins to form at stage 22 with the dermal ossification of costal plates 1°–8° (Table 1). The diffuse and laminar centres of these plates surround the dorsal ribs II–IX. At stage 23 the costal plate 1° shows an anteromedial process that contacts the dorsal rib I (Figs 7B,8B and 9B). Dermal ossification of the neural plates (dorsal to the neural spines) and nuchal plate starts at stage 23 and ends after hatching (Table 1). The ossification pattern of neural plates has the following characteristics: (1) it begins with plate 3° and progresses posteriorly to plate 8° (variably within stage 23); and (2) at stage 25 ossification progresses anteriorly to the neural 2°. At stage 26 the shape of the nuchal plate is similar to that of the adults and dorsal ribs I and II are joined by means of the costal plate 1° (Figs 7C and 8C).

In subadults the distal region of the costal plates remains cartilaginous. The partial contact of the dorsal ribs with the peripheral plates delimits lateral fontanelles between the costal plates, ribs and peripheral plates (Figs 7D, 8D and

9C). The shape of the nuchal plate is already defined in subadults: it is pentagonal, longer than wide, and with short posterior margins. The studied subadult presents seven neural plates, one pygal and one suprapygal.

In adults small fontanelles persist at the level of the costal plates. In contrast to the subadult, the adult has six neural plates (Figs 7E and 8E). The first of these neurals contacts the first two costals, while in the subadult the first two costals contact with the first and second neurals. Thus, the first neural plate of the adults represents neurals I and II of the subadult that fused during development. The contact on the midline between pairs 6°–8° of the costal plates is identical in subadults and adults: in both cases the last neural plate contacts the anteromedial margin of costal plate 6°. The neural plate 1° of the adult is suboval (so are neurals 1° and 2° of the subadult taken together), neurals 2°–5° are hexagonal, and neural 6° is pentagonal, all with short anterior margins. Neural plates decrease in size toward the rear. The suprapygal plate is kidney-shaped and becomes sutured to the adjacent peripheral plates and to the costal 8°. In visceral view it shows a mark that indicates the suture with the posterior margin of the ilium. The pygal plate is rectangular and slightly notched posteriorly.

Plastron

At stage 19 dermal centres corresponding to each plastral plate are present (Fig. 11A; Table 1). The paired epiplastra ossify anteriorly to the entoplastron and afterwards they grow in a cephalic direction only. The hyoplastra and hypoplastra ossify from centres located at the level of the anteroventral and posteroventral margins of the axillar and inguinal pillars, respectively. The xiphiplastra ossify at the level of the 'anal' projections of the adult. At stage 21 a more intensely stain-positive umbrella-shaped area becomes evident within the entoplastron matrix (see Pectoral girdle). This area corresponds to the dermal ossification centre of the interclavicle. We consider the interclavicle and the entoplastron as different structures for two reasons: (1) the interclavicle ossifies two stages latter than the entoplastron; and (2) the adult interclavicle is clearly recognizable as a separate element within the entoplastron. At stage 22 there is general osseous growth of the plastral centres involving: (1) expansion of the horizontal surface area of the hyoplastra by means of medial interdigitations; (2) hypoplastra larger but still widely separated at midline because of the vitelline sac; and (3) 'anal' projections of the xiphiplastra evident and well developed anteromedially. At stage 23 the following changes occur: (1) epiplastra more ossified anteriorly and posteriorly, encircling the entoplastron; (2) hyoplastra more developed anteromedially, interdigitated and contacting the epiplastra; (3) hypoplastra more developed and interdigitated both with each other and with the xiphiplastra; (4) axillar and inguinal pillars contacting the carapace at level of the distal margin of dorsal ribs II and VI, respectively; and (5) xiphiplastra well

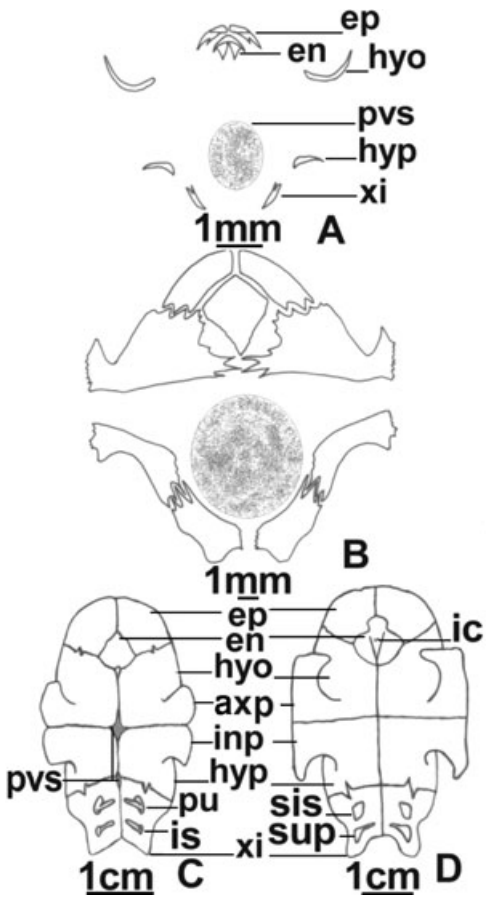

Fig. 11—Ventral views of the plastral bones of *Phrynops hilarii*. —**A**. Stage 19 (MLP R. 5321), —**B**. stage 26 (MLP R. 5331), —**C**. subadult (MLP R. 5337), and —**D**. adult (MLP Q. 026). Abbreviations: axp, axillar pillar; en, entoplastron; ep, epiplastron; hyo, hyoplastron; hyp, hypoplastron; ic, interclavicle; inp, inguinal pillar; is, ischium; pu, pubis; pvs, position of vitelline sac; sis, ischium suture; sup, pubis suture; xi, xiphiplastra.

ossified at level of anal projections but not interdigitated. At stages 25 and 26 there is a progress on the ossification of all plastral plates but with no significant structural changes (Fig. 11B).

In subadults extensive non-sutured areas are still present at the midline of hyoplastra and hypoplastra and at the anterior region of the xiphiplastra. These sutures are completely closed in adults (Fig. 11C). The xiphiplastra become sutured to the ischia and pubes. The axillar pillar is sutured to the costal plate 1° and the inguinal pillar is sutured to costals 5° and 6°. The latter suture is small because of the lack of ossification of the distal end of the costals in subadults, although this ossification is complete in adults.

In adults the well-developed axillar pillar is sutured to the costal 1° and to peripheral plate 3° (anterior sector) and 4° (posterior sector) (Fig. 11D). This suture takes the same shape as the dorsal rib II which it overlies, and occupies

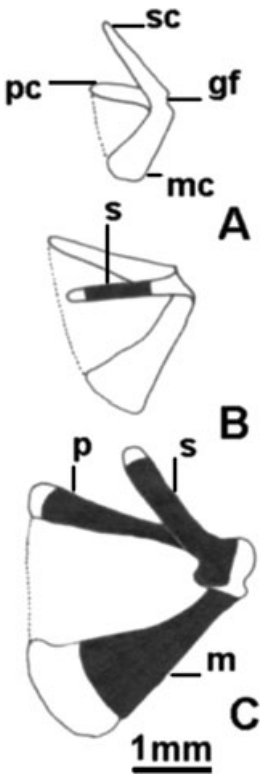

Fig. 12—Dorsal views of the right pectoral girdle of *Phrynops hilarii*. —**A**. Stage 19 (MLP R. 5321), —**B**. stage 21(MLP R. 5322), and —**C**. stage 23 (MLP R. 5326). Black areas are bone. White areas are cartilage. The dashed line shows the position of the epicoracoid ligament. Abbreviations: gf, glenoid fossa; m, metacoracoid; mc, metacoracoid cartilage; p, precoracoid; pc, precoracoid cartilage; s, scapula; sc, scapular cartilage.

two-thirds of the width of the respective costal plate. The inguinal pillar is attached to the carapace by a suture that is less extended medially and more extended anteroposteriorly compared with that of the axillar pillar. This suture spans the distal portion of costal 5°, posterior region of dorsal rib VI, anterolateral margin of costal 6°, and posterior and anterior edges of peripherals 7° and 8°.

Pectoral girdle

At stage 19 it is represented by single cartilaginous primordium for each half of the girdle. Each primordium bears anterior, posterior and dorsal arms (Fig. 12A). At stage 21 perichondral ossification of the scapula begins at the middle portion of the dorsal arm of the primordium (Fig. 12B; Table 1). At stage 21 dermal ossification of the interclavicle occurs (see Plastron above). At stage 22 the scapula is almost completely ossified and there is a well-developed perichondral centre in the posterior arm of the primordium representing the metacoracoid. All specimens at this stage show the precoracoid perichondral centre in the central portion of the anterior arm of the primordium (Table 1). At stage 23 the three bones of the girdle are completely ossified except for their distal tips and the glenoid cavity area (Fig. 12C). This morphology persists until stage 26 with no observable changes.

Subadults and adults show the following features: (1) ossified glenoid cavity, and (2) distal portions of scapula and metacoracoid remain cartilaginous and well developed forming the suprascapular and epicoracoid cartilages.

Forelimb and manus

At stage 19 the humerus, radius and ulna are already perichondrally ossified at mid-shaft (Fig. 13A). The ulna articulates with the intermedium and the ulnare, both cartilaginous. The ulnare articulates with a well-chondrified pisiform. The clearly separated central carpals III and IV are well chondrified. Central carpal IV articulates with the ulnare and intermedium, and central carpal III articulates broadly with the distal margin of the intermedium. The digital arch is composed of well-chondrified distal carpals I–V and digits I–V (phalangeal formula 2 : 3 : 3 : 3 : 3). A preaxial element is present in line with the distal carpals and articulated with the distal carpal I. We considered this element as a prepollex (following Holmgren 1933). The zeugopodial and stylopodial elements are completely ossified by stage 22. Perichondral ossification of metacarpals II–IV also begins at this stage (Table 1). Although the series of phalanges are incompletely ossified in some stage 25 specimens, all phalanges begin perichondral ossification in the more advanced stage 23 embryos (Fig. 13C). Based on the variation observed on these stages, we determined that ossification patterns for the phalanges may proceed: (1) proximo-distally (for digit I); (2) disto-proximally (for digit II); and (3) in digits III–V ossification starts at the second phalanx, continues at the distal phalanx and ends at the proximal one. In all cases, ossification of each phalanx proceeds from the diaphysis toward both epiphyses. Although the phalanges and metacarpals are completely ossified by stage 26 most carpal elements remain cartilaginous (Fig. 13D; Table 1). Only the intermedium and the ulnare are endochondrally ossified in advanced specimens.

In subadults the humerus represents slightly more than half of the total limb length, followed in relative size by the autopodium and lastly the zeugopodium (Fig. 13E). The humerus is completely ossified with a slightly preaxial, terminal proximal head. Anterior and posterior surfaces for muscular attachment are present at each side of the proximal head; the posterior surface is twice as large as the anterior one. The ulna is somewhat broadened distally and subequal to the radius. The autopodium (except for the pisiform and prepollex) is completely ossified. The intermedium and ulnare are largest and subequal, with distal carpal IV and central carpals III–IV following in size. The remaining distal carpals are the smallest among the carpal elements. Both central carpals remain sutured.

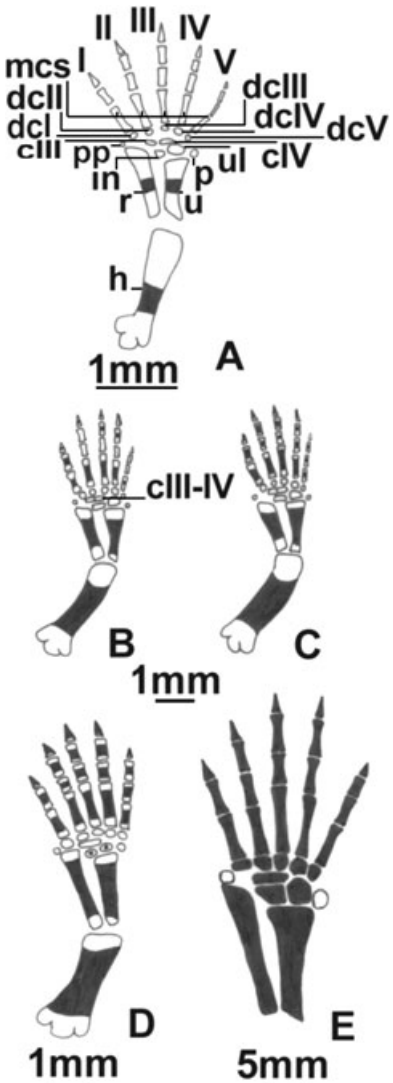

Fig. 13—Dorsal views of the right forelimb of *Phrynops hilarii*. —**A**. Stage 19 (MLP R. 5321), —**B**. stage 23 (MLP R. 5324), —**C**. stage 23 advanced (MLP R. 5326), —**D**. stage 26 (MLP R. 5331), and —**E**. subadult (MLP R. 5337). White areas are cartilage. Black areas are bone. Abbreviations: I–V, digits I–V; cIII, third central; cIV, fourth central; cIII–IV, centrals III and IV sutured; dcI–V, distals I to V; h, humerus; in, intermedium; mcs, metacarpals; p, pisiform; pp, prepollex; r, radial; u, ulnar; ul, ulnare.

In the adult the previously described morphology persists. In addition, the prepollex and pisiform are ossified.

Pelvic girdle

At stage 19 the pelvic girdle consists of a cartilaginous primordium with the following characteristics (Fig. 14A,B): (1) epipubis and pectineal processes projected anteroventrally from the pubic portion of the primordium; (2) thyroid

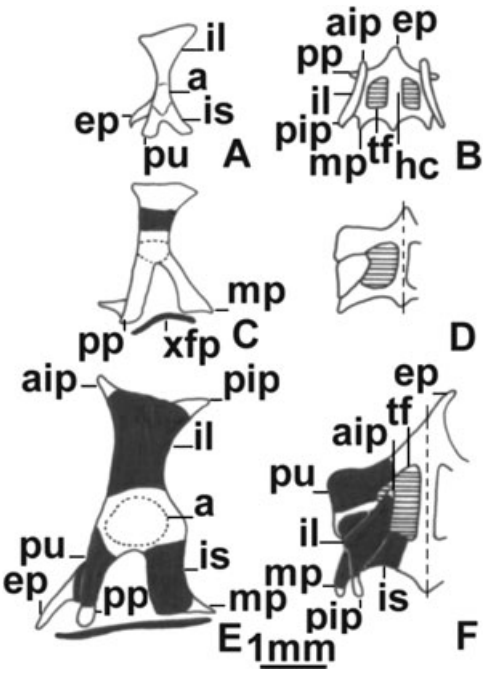

Fig. 14—Pelvic girdle of *Phrynops hilarii*. —**A**, **B**. Stage 19 (MLP R. 5321); —**C**, **D**. stage 21 (MLP R. 5322); and —**E**, **F**. stage 23 (MLP R. 5326). —**A**, **C**, **E**. Lateral views from left side, —**B**, **D**, **F**. dorsal views (left side only for stages 21 and 23). White areas are cartilage. Black areas are bone. Abbreviations: a, acetabulum; aip, anterior ilial process; ep, epipubis; hc, hypogastroid cartilage; il, ilium; is, ischium; mp, metischial process; pip, posterior ilial process; pp, pectineal process; pu, pubis; tf, thyroid fenestra; xfp, xiphiplastra.

fenestra divided into left and right portions by the hypogastroid cartilage; (3) metaischiadic processes projected posterolaterally from lateral margin of ischiadic portion of the primordium (longer than pectineal processes); (4) hypogastroid cartilage projected posteriorly to the primordium as a well-developed process; (5) iliac portion of primordium T-shaped because of anterodorsal and posterodorsal (relative to acetabulum) processes; and (6) well-defined acetabulum. At stage 21 perichondral ossification of ilia, ischia and pubes begins (Table 1; Fig. 14C,D). At stage 22 ilia are completely ossified and at stage 23 ischia and pubes complete their ossification (Fig. 14E,F). The only portions of the pelvic girdle still cartilaginous at this stage are acetabulum, pectineal process, metaischiadic processes, anterior and posterior iliac processes, and hypogastroid cartilage. More advanced individuals at this stage show contact between the ilium and the last costal plate. No changes are recorded during stages 25 and 26.

In subadults, the pelvic girdle is more ossified because of the ossification of the pectineal process and anterior and posterior iliac processes (the latter involved in the suture to the carapace). These bones become sutured to the xiphiplastra

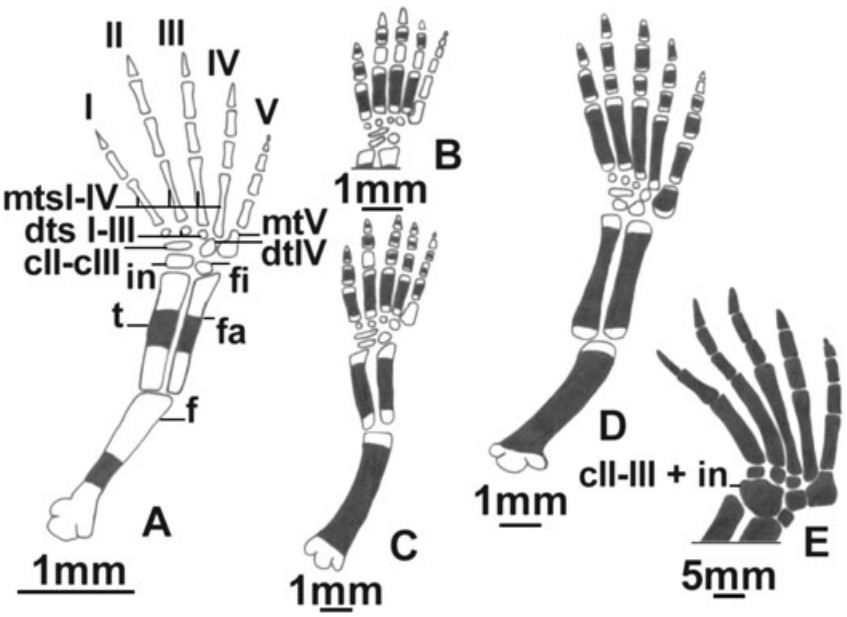

Fig. 15—Dorsal views of the right hindlimb of *Phrynops hilarii*. —**A**. Stage 19 (MLP R. 5321), —**B**. stage 23 (MLP R. 5324), —**C**. stage 23 advanced (MLP R. 5326), —**D**. stage 26 (MLP R. 5331), and —**E**. subadult (MLP R. 5337). White areas are cartilage. Black areas are bone. Abbreviations: I–V, digits I–V; cII–cIII, centrals II and III fused; dts I–III, distal tarsals I–III; dtIV, distal tarsal IV; f, femur; fa, fibula; fi, fibulare; in, intermedium; mts I–IV, metatarsals I–IV; mtV, metatarsal V ('hooked bone'); t, tibia.

whereas ilia become sutured to the last costal plate laterally and to the suprapygal plate medially. The ilium contacts with the last two ('sacralized') dorsal ribs and with the sacral ribs. The ilium contributes most to the acetabulum followed by pubis and ischium with very similar degree of participation.

In adults the only cartilaginous areas of the pelvic girdle are the epipubis, hypogastroid cartilage and metaischiadic processes.

Hind limb and pes

The stylopodial and zeugopodial elements are first to ossify. By stage 19 femur, tibia and fibula are perichondrally ossified at mid-shaft (Fig. 15A). At this stage the intermedium and fibulare are well chondrified. The basipodium presents an elongated central interpreted as fusion of centrals II and III because of its size and position, and four distal tarsals. The digital arch comprises four metatarsals that show normal development (metatarsals I–IV) and a fifth metatarsal (hooked) arranged almost in a series with the distal tarsals. Distal tarsal IV is in line with the fibulare and twice the size of the other distal tarsals. Distal tarsals I–III articulate with the distal surface of the central. The phalangeal formula is 2 : 3 : 3 : 3 : 5. The perichondral ossification of metatarsals I and IV begins at stage 21. Ossification of metatarsals continues at stage 22 with metatarsals II and III (Table 1). At stage 23 the perichondral ossification of the phalanges begins (Fig. 15B,C; Table 1). The ossification of digit I phalanges could not be elucidated because these elements are completely ossified in all stage 23 specimens. Ossification of digit II proceeds from distal to proximal phalanges, and at this stage only phalanges 2° and 3° are ossified. For digits III and IV ossification begins at the phalanx 2°, continues at the distal one and ends at the proximal one. All these phalanges are ossified in the more advanced specimen of this stage. Ossification of digit V phalanges proceeds from proximal to distal and at stage 23 the phalanges 4° and 5° remain cartilaginous. Ossification of each phalanx progresses from diaphysis to epiphyses. At stage 26 the basipodium is still cartilaginous and digits I–V are completely ossified (Fig. 15D). The fifth phalanx of digit V ossifies after hatching (Table 1).

In subadults all the elements are completely ossified (Fig. 15E). The longest segment with respect to overall limb length is the stylopodium with the autopodium as close second. The zeugopodium is slightly shorter than the autopodium. The proximal head of the femur is markedly terminal with two areas for muscle insertion at each side, of which the posterior is largest. Tibia and fibula are subequal. The fibula has a broadened distal epiphysis whereas the tibia has a broader proximal epiphysis. The largest autopodial element is the intermedium, followed by distal tarsal IV, centrals and fibulare, whereas the remaining elements are subequal and smaller. The digits show no changes with respect to stage 26, except by the perichondral ossification of the phalanx 5° of digit V.

In adults the only modification with respect to subadults is the formation of a suture among the intermedium, fibulare and centrals (Fig. 16).

Discussion

The development of skeletal elements is an important tool to support proposed homologies between structures, study

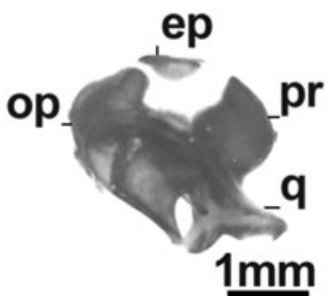

Fig. 16—Lateral view from the right otic capsule and the quadrate of *Phrynops hilarii* at stage 23 (MLP R. 5326). Abbreviations: ep, epiotic; op, opisthotic; pr, prootic; q, quadrate.

their variability, and understand morphological and phylogenetic patterns. In spite of this, in the case of Testudines, there exists a wide temporal gap between the pioneering studies made at the end of the 19th century and in the early 20th century (see review of these studies in de Beer 1937), and the series of recent works that provide complete skeletal descriptions for previously unknown turtle taxa (Kuratani 1987, 1989; Rieppel 1993a; Sheil 2003, 2005; Sheil and Greenbaum 2005; Tulenko and Sheil 2007). The abovementioned studies involve cryptodiran genera of the families Chelydridae, Cheloniidae, Dermochelyidae, Emydidae and Trionychidae.

This study represents the first comprehensive contribution to the knowledge of the development of skeletal structures for pleurodiran turtles, and it is principally focused on features of the chondrocranium as well as cranial and postcranial ossification patterns that differ from those described or from other groups of cryptodiran turtles. Among Testudines the chondrocranium is known for *Chrysemys picta* (de Beer 1937), *Emys orbicularis* (de Beer 1937) and *Trachemys scripta* (Tulenko and Sheil 2007) (Emydidae); *Apalone spinifera* (Trionychidae; Sheil 2003); *Chelydra serpentina* (Sheil 2005; Sheil and Greenbaum 2005) and *Macrochelys temminckii* (Sheil 2005) (Chelydridae); *Dermochelys coriacea* (Dermochelyidae; de Beer 1937), *Caretta caretta* (Kuratani 1987, 1989), *Chelonia mydas*, *Lepidochelys olivacea*, and *Eretmochelys imbricata* (de Beer 1937) (Cheloniidae); *Emydura subglobossa* (Chelidae; Esswein 1992); and *Podocnemis unifilis* (Pelomedusidae; Esswein 1992). In general, the paucity of data on the fully formed chondrocranium precludes the drawing of robust conclusions. An overall consideration of the chondrocranium of Testudines shows few variations within a remarkably homogeneous morphology. In other words, the chondrocranial features of turtles are quite similar to each other in relation to the variation that occurs within other vertebrate groups such as Anura (see Haas 2003). In fact, the comparison of the published information for the 13 abovementioned Testudines genera with the chondrocranial features of *P. hilarii* offers few noteworthy points. The nasal capsule of *P. hilarii* appears simple when compared with that of cryptodirans. The antorbital plane of *P. hilarii* lacks the ectochoanal and rostral processes that were described for most cryptodirans (e.g. Sheil 2003, 2005; Sheil and Greenbaum 2005) and for the pleurodiran *Emydura subglobossa* (Esswein 1992).

Phrynops hilarii lacks two features that are present in all known cryptodirans: the caudal projection of the tectum synoticum and the ascending process of the pterygoquadrate cartilage. The ascending process is also absent in the pleurodirans *Emydura subglobossa* (Chelidae) and *Podocnemis unifilis* (Pelomedusidae) (Esswein 1992). Although there is no mention on the caudal projection of the tectum synoticum of *Emydura subglobossa* in the Esswein (1992) paper, in the illustration of the lateral view of this species, the tectum synoticum lacks a clear caudal projection. Within turtles, the absence of both ascending process and caudal projection of the tectum synoticum are features unique to pleurodirans. If we compared the pleurodirans with other tetrapod groups the ascending process is absent in snakes (Scrocchi *et al.* 1998; Rieppel and Zaher 2001) and birds (de Beer 1937), it is well-developed in lizards (Lobo *et al.* 1995; Lions and Alvarez 1998), lissamphibians (Haas 2003) and mammals (de Beer 1937), but appears reduced in crocodilians (de Beer 1937). If we consider also that the ascending process appears first in ripidistians (Vorobyeva 2003), the most plausible hypothesis is that the absence of the ascending process is a secondary loss that occurred independently in many groups of tetrapods. The presence of the caudal projection of the tectum synoticum is difficult to assess in the descriptions of the chondrocranium of most tetrapod groups. Within sauropsids, the caudal projection of the tectum synoticum is a feature unique of cryptodirans because it is absent in pleurodirans (Esswein 1992; present paper) and all groups of extant sauropsids (de Beer 1937; Lobo *et al.* 1995; Lions and Alvarez 1998; Scrocchi *et al.* 1998; Rieppel and Zaher 2001).

As discussed in the previous paragraphs, *P. hilarii* lacks the ascending process of the pterygoquadrate cartilage. This process was described in other turtles such as *Apalone spinifera*, *Chelydra serpentina*, *Chrysemys picta*, *Emys orbicularis*, *Macrochelys temminckii* and *Trachemys scripta*; although there is no mention of this process in other published descriptions, this cannot be taken to imply that it is absent (de Beer 1937; Sheil 2003, 2005; Tulenko and Sheil 2007). Gaffney (1979; pp. 97–99) discussed the presence and degree of development of the epipterygoid in different groups of cryptodirans, and attributed the absence of this bone in some turtles (e.g. *Dermochelys coriacea*) to secondary loss of its ossification centre. Gaffney (1979) considered the ascending process and the pterygoid process as the same within the pterygoquadrate cartilage, as other authors did (e.g. de Beer 1937; Sheil 2003, 2005). Whereas the pterygoid process runs parallel to the floor of the neurocranium, the ascending process is perpendicular, describing an almost vertical trajectory between the pterygoquadrate cartilage and the antotic pillar. The absence of the ascending process was not reported for

cryptodirans and; as noted previously, the fact that some authors fail to mention this process does not necessarily imply its absence. The epipterygoid is present in stem turtles and its absence in some extant ones may be considered a secondary loss. We think that the absence of epipterygoid may be explained by at least two reasons: (1) the absence of ascending process as occurs in *P. hilarii* and in some cryptodirans (e.g. *Dermochelys*), and (2) the absence of the epipterygoid ossification centre. Probably, the lack of epipterygoid in other pleurodirans (e.g. *Hydromedusa*, *Phrynops sensu lato*, *Chelus*, *Chelodina*) should be explained by the absence of an ascending process as in *P. hilarii*. We think that future papers should establish clearly if the lack of epipterygoid is the result of the absence of the ascending process or the absence of the respective ossification centre.

The nasal and splenial bones are absent in all cryptodirans and in pelomedusid pleurodirans. The nasals and splenials of *P. hilarii* ossify at early stages (stage 19; Table 1). Conversely, bones absent in pleurodirans but usually present in cryptodirans such as the quadratojugals also form early in development (see Sheil 2003, 2005). These patterns differ from those known for other groups in which the bones that appear late in development are usually the ones that are frequently absent (e.g. quadratojugals and columella in the Anura) (Trueb 1985).

The scleral ossicles are plates of bone formed on the sclerotic ring of the eyeball. They are a plesiomorphy of several extant sauropsid groups (Franz-Odendaal 2006). Despite their general presence in turtles, mention of their development was usually omitted in the accounts of skeletal development of turtles (Andrews 1996; Franz-Odendaal 2006), in contrast with the detailed studies available for birds (Nelson 1942; Hall 1981). Andrews (1996) studied several cryptodirans and concluded that the scleral ossicles of this group develop by endochondral ossification. There is no mention of the development of the scleral ossicles in most studies about other cryptodirans and many sauropsids (Lobo *et al.* 1995; Abdala *et al.* 1997; Scrocchi *et al.* 1998; Rieppel and Zaher 2001; Sheil 2003, 2005; Arias and Lobo 2006). Franz-Odendaal (2006) restudied *Chelydra serpentina* and concluded that, contrary to the interpretation by Andrews (1996), the ossicles develop intramembranously, as in most sauropsids. Our observations on *P. hilarii* agree with those of Franz-Odendaal (2006).

According to Gaffney (1979) the foramen intermaxillaris is an unpaired palatal opening defined primarily by the maxillae and with contributions of the vomer and/or the premaxillae. This opening is present in *Carettochelys* and most trionychids, but Sheil (2003) recognized a foramen intermaxillaris in his redrawing of the adult skull of *Macrochelys temminckii* published first by Gaffney (1979). The subadults and adults of *P. hilarii* possess two openings between the maxilla and the premaxilla. There are at least two possibilities for the homology of these foramina: (1) they correspond to the single adult foramen intermaxillaris; or (2) they are homologous to the adult foramina prepalatina. We consider herein that both names represent two conditions (paired or unpaired) for the same structure. The principal reason is that the coexistence in a single species of the foramen intermaxillaris and the foramina prepalatina was never reported (see illustrations on Gaffney 1979). In fact, Gaffney (1979) described the adult foramina prepalatina as the openings that conduct the anterior nasal artery from the palate to the nasal cavity whereas he did not provide data about the function for the foramen intermaxillaris. In addition, the foramen intermaxillaris and the foramina prepalatina open in the anterior region of the palate and the bones that delimit them are the same. We suggest the term foramen intermaxillaris for the adult paired or unpaired openings of the anterior region of the palate. With respect to the term foramina prepalatina, we propose to restrict the term to the chondrocranial openings that conduct the anterior nasal artery in the embryos.

With respect to the entoglossal bones, they are ossified in the adults of *P. hilarii*. Unfortunately, we did not find published data about the entoglossal bones of any turtle (e.g. Gaffney 1979; Sheil 2005; Sheil and Greenbaum 2005). Sheil (2003) mentioned that the entoglossum remains cartilaginous in the adults of *Apalone spinifera*. De Beer (1937) did not mention the development of the entoglossal bones in the species of cryptodirans that he studied. There is no mention of the entoglossal bones in other papers about the cranial development of different species of Lepidosauria and Archosauria (Rieppel 1992, 1993b; Lobo *et al.* 1995; Abdala *et al.* 1997; Scrocchi *et al.* 1998; Rieppel and Zaher 2001; Arias and Lobo 2006).

We observed some features in the osteogenesis of *P. hilarii* that question some statements currently generalized for all Testudines. Such is the case of the absence of the epiotic bone. Extant turtles presumably lack this bone because Gaffney (1979) wrote: 'contrary to Shaner (1926; p. 358), there is no evidence that epiotics exist in turtles ...' The recently published studies about the ossification sequence of many turtles such *Apalone spinifera*, *Chelydra serpentina* and *Macrochelys temminckii* support Gaffney's view about the absence of epiotics in turtles (Sheil 2003, 2005; Sheil and Greenbaum 2005). However, this is not the case for *P. hilarii*, a species that possesses the perichondral centre of the epiotic placed on the dorsomedial wall of the otic capsule at stage 23 (Fig. 16). In this species, the epiotic centre becomes fused with the supraoccipital in all embryos at stage 24. To detect the epiotic before fusion with the supraoccipital is not easy. Taking into account present knowledge, the absence/presence of the epiotic seems to be variable in Testudines. We think that this variability should be acknowledged by considering developmental data sets of more taxa in a phylogenetic context.

Phrynops hilarii presents the same vertebral formula as all the 'Recent' turtles: 8 CVs, 10 DVs, 2 SVs, and a variable number of CaVs. In Pleurodira, the last DVs are functionally

sacralized (Hoffsteter and Gasc 1969). The sacral region of *P. hilarii* is formed by four vertebrae: the two SVs and DVs IX and X. In all the stages studied we observed that the two sacral vertebrae reach the ilium by means of two short cartilaginous ribs (ossified in adults). Instead, the dorsal ribs IX and X become 'sacralized' later in development, just at the moment when the ilium sutures to the carapace.

The number of CaVs is known to vary among turtles. We observed the following variation in the number of CaV among the different stages of the development *P. hilarii*: stage 19 ($n = 1$; 20 CaVs); stage 21 ($n = 1$; 22 CaVs); stage 22 ($n = 1$; 22 CaVs); stage 23 ($n = 4$; 18–20 CaVs); stage 25 ($n = 3$; 19–20 CaVs); stage 26 ($n = 6$; 19–20 CaVs); subadults and adults ($n = 3$; 17 CaVs). Although the data are not clear at all, the CaVs show a clear reduction in number since stage 23.

Vertebral ossification of *P. hilarii* progresses from anterior to posterior within each region. In most regions, each vertebra begins to ossify at the neural arch; the exception is the caudal region, where the vertebral centrum is the first part to ossify. Hoffsteter and Gasc (1969; p. 206) recorded that in Squamata and Testudines the condyle of each vertebra is formed by the intercentrum. As first observed by Sheil (2003, 2005), and contrary to Hoffsteter and Gasc (1969), in *P. hilarii* the vertebral condyle of each vertebra is formed by growth of the centrum without contribution from the intercentrum, which never forms except in the atlas (e.g. Sheil 2003, 2005). The presence of two atlantic centra (centrum and intercentrum) independent from the structure of the atlas–axis complex seems to be a unique character of Testudines (in the context of the Amniota). Within Testudines, the relationship between centrum and intercentrum shows at least two possible conditions. In some taxa (such as *Phrynops hilarii*) both elements are sutured, whereas in other genera (e.g. *Hydromedusa tectifera*) they are fused to each other (Bona and de la Fuente 2005).

At carapace level, the first elements to ossify are the dermal plates of the plastron, followed by the costal plates, neurals III–VIII and nuchal plate, and neurals II–IX. The union between the dorsal ribs I and II with the first costal plate and the contact between ilium and dorsal carapace occurs later during ontogeny (stage 26). The suture between ilium and carapace is a derived feature of Pleurodira.

The beginning and progress of ossification of the neural plates is the same as for the respective neural arches, at least for neurals III–VIII. The number of neurals shows intraspecific variation in different species of turtles. In *P. hilarii*, the number of neural plates in adults is variable (the minimum reported is six), but we observed that in all studied embryos herein, eight neural plates form and then fuse during posthatching. At least in the species studied here, the variation in number of neural plates of adults is explained by a process of ontogenetic fusion.

The autopodium of turtles shows great variability in terms of phalangeal formulae and with respect to the arrangement of carpal and tarsal bones (Boulenger 1889; Holmgren 1933; Walker 1973; Gaffney 1990; Sheil 2003, 2005; Hitschfeld *et al.* 2008; Sánchez-Villagra *et al.* 2008). Additionally, the modifications that occurred during turtle evolution remain poorly described (Sánchez-Villagra *et al.* 2007). Characters from the autopodium such as phalangeal formula, fusions and reductions of bones, were not frequently used in the phylogenetic reconstruction of turtle relationships. In the case of pleurodirans, descriptions of the autopodium are scarce, and homology proposals with the elements present in other taxa are rare. From our observations on the development of *P. hilarii*, we found that carpal elements of this species are arranged in three proximal (intermedium, ulnare and pisiform), two centrals (III and IV), and five free distal carpals, and a preaxial element aligned with the distal series and in contact with the distal carpal I, that we considered as a *prepollex* according to Holmgren (1933) (see Burke and Alberch 1985 for critics to this view). The phalangeal formula described herein for the manus of *P. hilarii* agrees with that described for Sánchez-Villagra *et al.* (2007) for the same species: 2 : 3 : 3 : 3 : 3. Additionally, these authors considered that this phalangeal formula is the basal condition for the manus of Pleurodira. Sánchez-Villagra *et al.* (2007) considered that the presence of pisiform and prepollex, as well as the number of central (ranging between 0 and 3) and distal (ranging between 3 and 5) carpals, varies within Pleurodira.

The proximal tarsals of the pes in adults of *P. hilarii* (intermedium and fibulare) are sutured to the single central (formed from fusion of centrals II and III). This complex of elements articulates with distal tarsals I–IV. As demonstrated by previous works, the fifth digit of the turtles is formed from a postaxial condensation, formed independently of the digital arch (Burke and Alberch 1985). Based on our observations, and in line with proposals made by other researchers (Burke and Alberch 1985; Lee 1997; Arias and Lobo 2006), we consider that the 'hooked' bone in the fifth digit is a metatarsal V, and not a distal tarsal V. The most common view about the homology of the hooked bone is that it represents the fusion of the distal tarsal V and the fifth metatarsal (Holmgren 1933; Robinson 1975; Gauthier *et al.* 1988; Sánchez-Villagra *et al.* 2007). However, this kind of fusion was never demonstrated in studies of the tarsal development of Testudines and Lepidosauria, two groups that possess hooked bones (e.g. Burke and Alberch 1985; Sheil 2003; Arias and Lobo 2006; Sánchez-Villagra *et al.* 2008; present work). The formation of the hooked bone as revealed by the above-mentioned studies is as follows: (1) it chondrifies as a single, homogeneous primordium, situated laterally to the metatarsal IV; (2) it ossifies in the above-mentioned primordium from a single ossification centre (when central carpals or tarsals are fused, each element ossifies from separate centres located within the single cartilaginous element); and (3) perichondral ossification of the hooked occurs as in all digital elements (metapodium and phalanges) contrary to the endochondral

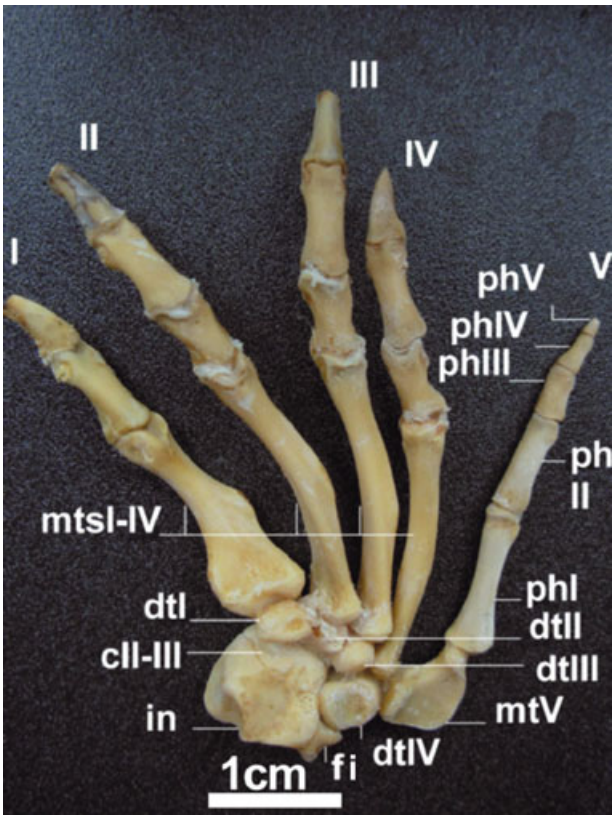

Fig. 17—Dorsal view of the right pes of an adult male of *Phrynops hilarii* (FML 14953). Abbreviations: ph I–V, phalanges I–V. Other abbreviations as in Fig. 15.

ossification of basipodial elements (carpals and tarsals). This third theory was never indicated in previous works, but it seems important in this context. In fact, the perichondral ossification of the hooked is one of the features that better support the interpretation of the hooked as metatarsal V. Finally, the hooked bone of turtles does not articulate with the proximal tarsals, as would be expected if it was a fifth distal tarsal (see Sheil 2003 fig. 9; 2005 fig. 12; Sánchez-Villagra *et al*. 2007 fig. 1; present work, Fig. 17).

The fifth digit of the pes of *P. hilarii* has five phalanges, contrary to previous descriptions made for this species (Sánchez-Villagra *et al.* 2007). The count of phalanges of the fifth digit is obviously conditioned by the interpretation of the hooked bone. However, independently of this fact, *P. hilarii* possesses an additional and previously unknown small distal phalanx (see Fig. 17), which makes the phalanx formula of this species 2 : 3 : 3 : 3 : 5. As usual in this group of turtles, this phalanx lacks a claw and is easily removed in preparations of dried materials. We observed this small fifth phalanx from the first stage examined (stage 19) and consequently we prepared the dried skeletons with special care to avoid the loss of this element. Future studies will reveal if this feature is unique to *P. hilarii*, or shared by all *Phrynops sensu lato*, or even characterizes more inclusive groups such as Chelidae or Pleurodira.

Acknowledgements

L. Alcalde acknowledges CONICET for the Postdoctoral Scholarship 2007. The present paper constitutes the ILPLA Scientific Contribution 815 (CCT La Plata-CONICET-UNLP). We are grateful to R. Herrera and J. Pipi, who gave us most of the embryos used for the study, to the curators of the Museo de La Plata (J. D. Williams) and to the Fundación Miguel Lillo (S. Kretzschmar) Herpetological Collections for allowing us to study the adult specimens under their care.

Appendix I

Double-stained and cleared embryos: stage 19 (MLP R. 5321); stage 21 (MLP R. 5322); stage 22 (MLP R. 5323); stage 23 (MLP R. 5324–5327); stage 25 (MLP R. 5328–5330); stage 26 (MLP R. 5331–5336).

Subadult male (carapace length 192 mm) collected at Los Talas (Berisso, La Plata, Buenos Aires province, Argentina) on February 2002, dry postcranial axial skeleton and carapace; cranium, girdles and limbs double-stained and cleared (MLP R. 5337).

Adult male (carapace length 302 mm) collected at Entre Rios province (Argentine) on 14 June 1951, dry skeleton (without autopodium) (MLP Q. 026).

Adult male (carapace length 320 mm) from unknown locality, entire dry skeleton (FML 14953).

References

Abdala, F., Lobo, F. and Scrocchi, G. 1997. Patterns of ossification in the skeleton of *Liolaemus quilmes* (Iguania: Tropiduridae). – *Amphibia – Reptilia* **18**: 75–83.

Andrews, K. 1996. An endochondral rather than a dermal origin for scleral ossicles in cryptodiran turtles. – *Journal of Herpetology* **30**: 257–260.

Arias, F. and Lobo, F. 2006. Patrones de osificación en *Tupinambis merianae* y *Tupinambis rufescens* (Squamata: Teiidae) y patrones generales en Squamata. – *Cuadernos de Herpetología* **20**: 3–23.

de Beer, G. R. 1937. *The Development of the Vertebrate Skull*. The University of Chicago Press, Chicago & London.

Bever, G. S. 2008. Comparative growth in the postnatal skull of the extant North American turtle *Pseudemys texana* (Testudinoidea: Emydidae). – *Acta Zoologica (Stockholm)* **89**: 107–131.

Bona, P. and de la Fuente, M. S. 2005. Phylogenetic and paleobiogeographic implications of *Yaminuechelys maior* (Staesche, 1929) new comb., a large long necked chelid turtle from the Early Paleocene of Patagonia, Argentina. – *Journal of Vertebrate Paleontology* **25**: 569–582.

Boulenger, G. A. 1889. *Catalogue of the Chelonians, Rhynchocephalians and Crocodiles in the British Museum (Natural History)*. British Museum Natural History, London.

de Broin, F. 1988. Les Tortues et le Gondwana. Examen des rapports entre le fractionnement du Gondwana et la dispersión géographique des Tortues pleurodires á partir du Crétacé. –

Stvdia Geologica Salmanticensia, Stvdia Palaeocheloniologica **2**: 103–142.

Burbidge, A. A., Kirsch, J. A. and Main, A. R. 1974. Relationships within the Chelidae (Testudines: Pleurodira) of Australia and New Guinea. – *Copeia* **1974**: 392–409.

Burke, A. 1989. Development of the turtle carapace: implications for the evolution of a novel bauplan. – *Journal of Morphology* **199**: 363–378.

Burke, A. C. and Alberch, P. 1985. The development and homology of the chelonian carpus and tarsus. – *Journal of Morphology* **186**: 119–131.

Crumly, C. R. and Sánchez-Villagra, M. R. 2004. Patterns of variation in the phalangeal formulae of land tortoises (Testudinidae): developmental constraint, size and phylogenetic history. – *Journal of Experimental Zoology*: *Molecular Development and Evolution* **302**: 134–146.

Esswein, S. E. 1992. Zur phylogenetischen und ontogenetischen Entwicklung des akinetischen Craniums des Schildkrötten. In *Naturliche Konstructionen Natural Structures, Principles, Strategies, and Models in Architecture and Nature Part II*, pp. 51, 55. Sonderforschungbereich 230. Universität Stuttgart und Universität Tubingen, Mitteilungen des Sonderforschungbereich, Stuttgart–Tubingen.

Fabrezi, M. and Alberch, P. 1996. The carpal elements of anurans. – *Herpetologica* **52**: 188–204.

Franz-Odendaal, T. A. 2006. Intramembranous ossification of scleral ossicles in *Chelydra serpentina*. – *Zoology* **109**: 75–81.

Fujita, M. K., Engstrom, T. N., Starkey, D. E. and Shaffer, H. B. 2003. Turtle phylogeny: insights from a novel nuclear intron. – *Molecular Phylogenetics and Evolution* **31**: 1031–1040.

Gaffney, E. S. 1977. The side-necked turtle family Chelidae: a theory of relationships using shared derived characters. – *American Museum Novitates* **2620**: 1–28.

Gaffney, E. S. 1979. Comparative cranial morphology of recent and fossil turtles. – *Bulletin of the American Museum of Natural History* **164**: 67–376.

Gaffney, E. S. 1990. The comparative osteology of the Triassic turtle *Proganochelys*. – *Bulletin of the American Museum of Natural History* **194**: 1–263.

Gaffney, E. S. and Meylan, P. A. 1988. A phylogeny of turtles. In Benton, M. J. (Ed.): *The Phylogeny and Classification of the Tetrapods*, pp. 157–219. Clarendon Press, Oxford.

Gauthier, J., Estes, R. and Queiroz, K. 1988. A phylogenetic analysis of Lepidosauromorpha. In Estes, R. and Pregill, G. (Eds): *Phylogenetic Relationships of the Lizard Families*, pp. 15–98. Stanford University Press, Palo Alto CA.

Georges, A., Birrell, J., Saint, K. M., McCord, W. and Donnellan, S. C. 1998. A phylogeny for side-necked turtles (Chelonia: Pleurodira) based on mitochondrial and nuclear gene sequence variation. – *Biological Journal of the Linnean Society* **67**: 213–246.

Gilbert, S. F., Loredo, G. A., Brukman, A. and Burke, A. C. 2001. Morphogenesis of the turtle shell: development of a novel structure in tetrapod evolution. – *Evolution and Development* **3**: 47–58.

Greenbaum, E. and Carr, J. L. 2002. Staging criteria for embryos of the Spiny Softshell Turtle, *Apalone spinifera* (Testudines: Trionychidae). – *Journal of Morphology* **254**: 272–291.

Haas, A. 2003. Phylogeny of frogs as inferred from primarily larval characters (Amphibia: Anura). – *Cladistics* **19**: 23–89.

Hall, B. K. 1981. Specificity in the differentiation and morphogenesis of neural crest-derived scleral ossicles and of epithelial scleral papillae in the eye of the embryonic chick. – *Journal of Embryology and Experimental Morphology* **66**: 175–190.

Hall, B. K. 2005. *Bones and Cartilage: Development and Evolutionary Skeletal Biology*. Elsevier-Academic Press, London.

Hitschfeld, E., Auer, M. and Fritz, U. 2008. Phalangeal formulae and ontogenetic variation of carpal morphology in *Testudo horsfieldii* and *T. hermanii*. – *Amphibia – Reptilia* **29**: 93–99.

Hoffsteter, R. and Gasc, J. P. 1969. Vertebrae and ribs of modern reptiles. In Gasc, C. and Parsons, T. S. (Eds): *Biology of the Reptilia*, Vol. 1, pp. 201–309. Academic Press, London.

Holmgren, N. 1933. On the origin of the tetrapod limb. – *Acta Zoologica (Stockholm)* **14**: 185–295.

Joyce, W. G. 2007. Phylogenetic relationships of Mesozoic turtles. – *Bulletin of the Peabody Museum of Natural History* **48**: 3–102.

Kunkel, B. W. 1912. The development of the skull of *Emys lutaria*. – *Journal of Morphology* **23**: 692–694.

Kuratani, S. 1987. The development of the orbital region of *Caretta caretta* (Chelonia, Reptilia). – *Journal of Anatomy* **154**: 187–200.

Kuratani, S. 1989. Development of the orbital region of the chondrocranium in *Caretta caretta* – reconsideration of the vertebrate neurocranium configuration. – *Anatomischer Anzeiger* **169**: 335–349.

Lee, M. S. Y. 1997. The evolution of the reptilian hindfoot and the homology of the hooked fifth metatarsal. – *Journal of Evolutionary Biology* **10**: 253–263.

Lions, M. L. and Alvarez, B. B. 1998. Desarrollo del esqueleto de *Tropidurus etheridgei* (Iguania: Tropiduridae). – *Revista Española de Herpetología* **12**: 7–18.

Lobo, F., Abdala, F. and Scrocchi, G. 1995. Desarrollo del esqueleto de *Liolaemus scapularis* (Iguania: Tropiduridae). – *Bolletino Del Museo Regionale Di Scienze Naturali, Torino* **13**: 77–104.

Mabee, P. M. 2000. Developmental data and phylogenetic systematics: evolution of the vertebrate limb. – *American Zoologist* **40**: 789–800.

McCord, W. P., Joseph-Ouni, M. and Lamar, W. W. 2001. Taxonomic reevaluation of *Phrynops* (Testudines: Chelidae) with the description of two new genera and a new species of *Batrachemys*. – *Revista de Biologia Tropical* **49**: 715–764.

Nelson, N. M. 1942. The sclerotic plates of the white Leghorn chicken. – *Anatomical Record* **84**: 295–306.

Noonan, B. P. 2000. Does the phylogeny of pelomedusoid turtles reflect vicariance due to continental drift? *Journal of Biogeography* **27**: 1245–1249.

Rabl, C. 1910. *Bausteine Zu Einer Theorie der Extremitäten der Wirbeltiere. I. Teil*, p. 289. Verlag von Wilhelm Engelmann, Leipzig.

Rieppel, O. 1992. Studies on skeleton formation in reptiles. III. Patterns of ossification in the skeleton of *Lacerta vivipara* (Reptilia, Squamata). – *Fieldiana Zoology New Series* **68**: 1–25.

Rieppel, O. 1993a. Studies on skeleton formation in reptiles: patterns of ossification in the skeleton of *Chelydra serpentina* (Reptilia, Testudines). – *Journal of Zoology (London)* **231**: 487–509.

Rieppel, O. 1993b. Studies on skeleton formation in reptiles. V. Patterns of ossification in the skeleton of *Alligator mississipiensis* DAUDIN (Reptilia, Crocodylia). – *Zoological Journal of the Linnean Society* **109**: 301–325.

Rieppel, O. 1994. Studies on skeletal formation in reptiles: Implications for turtle relationships. – *Zoology* **98**: 298–308.

Rieppel, O. and Zaher, H. 2001. The development of the skull in *Acrochordus granulatus* (Schneider) (Reptilia: Serpentes), with special consideration of the otico-occipital complex. – *Journal of Morphology* **249**: 252–266.

Robinson, P. 1975. The functions of the hooked fifth metatarsal in lepidosaurian reptiles. – *Colloque International CNRS* **218**: 462–483.

Romer, A. S. 1956. *Osteology of Reptiles*. University of Chicago Press, Chicago.

Sánchez-Villagra, M. R., Winkler, J. D. and Wurst, L. 2007. Autopodial skeleton evolution in side-necked turtles (Pleurodira). – *Acta Zoologica (Stockholm)* **88**: 199–209.

Sánchez-Villagra, M. R., Ziermann, J. M. and Olsson, L. 2008. Limb chondrogenesis in *Graptemys nigrinoda* (Emydidae), with comments on the primary axis and the digital arch in turtles. – *Amphibia – Reptilia* **29**: 85–92.

Schumacher, G. H. 1973. The head muscles and hyolaryngeal skeleton of turtles and crocodilians. In Gasc, C. and Parsons, T. S. (Eds): *Biology of the Reptilia*, Vol. 4, pp. 101–199. Academic Press, London.

Scrocchi, G., Lobo, F. and Moreta, J. L. 1998. Desarrollo del esqueleto craneal de *Sibynomorphus turgidus* (Serpentes: Colubridae). – *Acta Zoologica Lilloana* **44**: 27–39.

Seddon, J. M., Georges, A., Bavesrstock, P. and McCord, W. 1997. Phylogenetic relationships of chelid turtles (Pleurodira: Chelidae) based on mitochondrial 12S rRNA gene sequence variation. – *Molecular Phylogenetics and Evolution* **7**: 55–61.

Shaffer, H. B., Meylan, P. and Mcknight, M. L. 1997. Test of turtle phylogeny: molecular, morphological, and paleontological approaches. – *Systematic Biology* **46**: 235–268.

Shaner, R. F. 1926. The development of the skull of the turtle, with remarks on fossil reptile skull. – *Anatomical Record* **32**: 343–367.

Sheil, C. A. 2003. Osteology and skeletal development of *Apalone spinifera* (Reptilia: Testudines: Trionychidae). – *Journal of Morphology* **256**: 42–78.

Sheil, C. A. 2005. Skeletal development of *Macrochelys temminckii* (Reptilia: Testudines: Chelydridae). – *Journal of Morphology* **263**: 71–106.

Sheil, C. A. and Greenbaum, E. 2005. Reconsideration of skeletal development of *Chelydra serpentina* (Reptilia: Testudinata: Chelydridae): evidence for intraspecific variation. – *Journal of Zoology (London)* **265**: 235–267.

Shubin, N. H. and Alberch, P. 1986. A morphogenetic approach to the origin and basic organization of the tetrapod limb. In Hecht, M. K. Wallace, B and Prance, G. T. (Eds): *Evolutionary Biology*, pp. 319–385. Plenum Press, New York.

Taylor, W. R. and Van Dyke, G. C. 1985. Revised procedures for staining and clearing small fishes and other vertebrates for bone and cartilage study. – *Cybium* **9**: 107–119.

Trueb, L. 1985. A summary of the osteocranial development in anurans with notes on the sequence of cranial ossification in *Rhinophrynus dorsalis* (Anura: Pipoidea: Rhinophrynidae). – *South African Journal of Science* **81**: 181–185.

Tulenko, F. J. and Sheil, C. A. 2007. Formation of the chondrocranium of *Trachemys scripta* (Reptilia: Testudines: Emydidae) and a comparison with other described turtle taxa. – *Journal of Morphology* **268**: 127–151.

Vickaryous, M. T. and Hall, B. K. 2006. Homology of the reptilian coracoid and reappraisal of the evolution and development of the amniote pectoral apparatus. – *Journal of Anatomy* **208**: 263–285.

Vorobyeva, E. 2003. Evolutionary Changes in the Dermal Skull of Recent Amphibians in Comparison with Ancestral Palaeozoic Crossopterygians. In Heatwole, H and Davies, M. (Eds): *Amphibian Biology*, **Vol. 5**, pp. 1497–1550. Surrey Beaty and Sons, Chipping Norton, Australia.

Walker, W. F. Jr. 1973. The locomotor apparatus of Testudines. In Gans, C and Parsons, T. S. (Eds): *Biology of the Reptilia*, **Vol. 4**, pp. 1–99. Academic Press, London.

Yntema, C. L. 1968. A series of stages in the embryonic development *of Chelydra serpentina*. – *Journal of Morphology* **125**: 219–251.

Zug, G. R. 1971. Buoyancy, locomotion, morphology of the pelvic girdle and hind-limb, and systematics of cryptodiran turtles. – *Miscellaneous Publications Museum of Zoology, University of Michigan* **142**: 1–98.